Theor Appl Climatol
DOI 10.1007/s00704-016-1854-2

ORIGINAL PAPER

Trend analysis of air temperature time series in Greece and their relationship with circulation using surface and satellite data: recent trends and an update to 2013

H. Feidas[1]

Received: 14 November 2015 / Accepted: 19 June 2016

Summary In this paper, the surface and lower tropospheric temperature trends in Greece and their relationship to the atmospheric circulation for the period 1955–2013 were examined, updating the study of Feidas et al. (Theor Appl Climatol 79:185–208, 2004) for data observed during the 12-year period 2002–2013. The trend analysis is based on a combination of three statistical tests. The trends are now examined for all the seasonal time series, new atmospheric circulation indices were added in the analysis, and maps with the spatial distribution of correlation between air temperature and atmospheric circulation were constructed and analysed. The series updated to 2013 for 18 stations reveal a clearer positive trend than that found for the period 1955–2001 on both the annual and the seasonal timescales. The warming signal detected only in summer in the study of Feidas et al. (Theor Appl Climatol 79:185–208, 2004) has now intensified and spread in other seasons. This warming appears to be mainly caused by the very high temperatures in the last decade (after 2004) of the record. At the national scale, there is now a match between surface temperature trends in Greece and Northern Hemisphere (NH) but only for summer, spring and annual time series, which are the only time series presenting a statistically significant warming trend in Greece. Satellite-induced lower tropospheric temperatures now show a statistically significant tropospheric temperature warming trend for the period 1979–2013, for both areas (Greece and NH). Lower tropospheric and surface air temperatures for the same period (1979–2013) show a very good agreement, with differences only in winter and summer for Greece. The influence of atmospheric circulation on the temperature variability in Greece was also examined using two more circulation indices: the Eastern Mediterranean Pattern Index (EMPI) and the North-Sea Caspian Pattern Index (NCPI). EMPI and especially NCPI explain better now the temperature variance in Greece, principally in winter. This connection, however, is not only developed during winter, as expected, but is also present for annual and other seasonal temperatures.

1 Introduction

According to the Fifth Assessment Report of the Intergovernmental Panel on Climate Change (IPCC) "climate warming is unequivocal, and since 1950, many of the observed changes are unprecedented over decades to millennia" (IPCC 2013). Analysis of global air temperature data indicates an average warming of 0.84 °C since 1860 with each of the last three decades being successively the warmest on record since 1850 (IPCC 2013).

The analysis of global climate variations, however, does not present a uniform spatial and temporal pattern (Jones and Moberg 2003). Regional climate variations often do not follow the typical global climate change pattern. For example, in the Mediterranean basin, many studies have found an evolution in air temperatures similar to that observed on the globe as a whole, namely, a cooling during the period 1955–1975 and an intense warming afterwards but with considerable variability over space and time (Piervitali et al. 1997; del Río et al. 2011). However, discrepancies arise in air temperature trends between the western and eastern Mediterranean. Whereas a distinct warming has been reported for the central and western Mediterranean (Piervitali et al. 1997; Brunet et al. 2007; del Río et al. 2011; Longobardi and Mautone 2015; Ageena et al.

✉ H. Feidas
hfeidas@geo.auth.gr

[1] Department of Meteorology and Climatology, School of Geology, Aristotle University of Thessaloniki, 54124 Thessaloniki, Greece

Published online: 07 July 2016

2014), trends in the eastern Mediterranean are not clear and consistent with the general temperature increase in the global or hemispheric scale. Early studies on air temperature trends in the Mediterranean detected a cooling in western Mediterranean for the period 1950–1990 (Parker et al. 1994; Sahsamanoglou and Makrogiannis 1992; Nicholls et al. 1996), whilst recent studies suggest either a general warming for some regions as Turkey (Türkeş et al. 2002) and Serbia (Bajat et al. 2015) or both warming and cooling for different seasons and parts of the country for regions such as Greece (Feidas et al. 2004; Nastos et al. 2011; Marougianni et al. 2012) and Egypt (Hasanean and Abdel Basset 2006).

Large-scale atmospheric circulation is an important element of the climate playing a key role in air temperature variability. Several studies have reported the linkages of atmospheric circulation patterns–expressed as climate teleconnection or circulation indices–with air temperature variability in the Mediterranean (Nastos et al. 2011; Knezevic et al. 2014; Kutiel and Brunetti 2010; Türkeş and Erlat 2009; Hatzaki et al. 2009; Feidas et al. 2004; Xoplaki et al. 2003; Kutiel and Maheras 1998).

At the national scale, Greece was found to be different from the rest of Europe in presenting a slight negative air temperature trend over the second half of the twentieth century, especially for winter (IPCC 1996; Proedrou et al. 1997; Retalis et al. 1998; Luterbacher et al. 2000; Mitchell and Hulme 2000; Feidas et al. 2004; Nastos et al. 2011; Marougianni et al. 2012). In a previous paper, Feidas et al. (2004) performed a trend analysis on the annual and seasonal air temperature time series of 20 weather stations in Greece for the period 1955–2001, as well as on satellite-induced temperature data of the lower troposphere for the period 1980–2001. Trend analysis was based on a combination of three statistical tests. The influence of atmospheric circulation on temperature variability in Greece was also investigated using three circulation indices. The results showed in general opposite–though not statistically significant–temperature trends for winter and summer resulting to a nearly zero overall trend in the annual temperatures. Temperature trends in Greece were found not to match the strong warming trends observed in the Northern Hemisphere. Finally, the Mediterranean circulation indices presented the best correlation with winter temperatures in Greece.

The aim of this paper is to analyse both the available temperature series in Greece and atmospheric circulation data, now updated with the 12-year period 2002–2013. Trend analysis is still based on a combination of three statistical tests. However, new results are obtained not only by building on previous analysis but also by introducing new approaches and data: a more strict approach was adopted to assess the homogeneity of the time series, trends are now examined for all the seasonal time series, new atmospheric circulation indices were included in the analysis, and maps with the spatial distribution of correlation between air temperature and atmospheric circulation were constructed and analysed.

2 Data and methodology

2.1 Surface air temperature data

The trend analysis used a complete version of the data set comprising mean monthly values of surface air temperature for 20 available stations in Greece, now updated to 2013. The selection of stations was first made based on the length, completeness and geographical coverage of the temperature data. These stations have the maximum common length of temperature records covering 59 years (1955–2013). Series were updated to 2013 using data mainly from the Hellenic National Meteorological Service, which has the most complete historical records of temperature measurements in Greece. Time series from two out of the twenty stations used in the study of Feidas et al. (2004) were removed due to their discontinued operation, whereas time series from two other stations became available and were added to the dataset. The geographical distribution of the stations is presented in Fig. 1 whereas their geographical coordinates and altitudes are shown in Table 1.

CLIMAT and SYNOP reports of the Hellenic National Meteorological Service (HNMS) were used to update the datasets up to 2013. Mean daily and monthly air temperature computation follows the same convention used in the data prior to 2004. CIMAT data have undergone basic quality checks on missing data and error detection made on site in order to ensure the highest possible standard of accuracy (WMO 2009). In addition, some station data quality controls are further performed in this study, including internal consistency check for unreasonable values and spatial consistency check with data from the neighbouring stations. Moreover, CLIMAT reports were double checked for missing values using SYNOP reports.

Occasional missing data and errors were present in only ten stations, not exceeding 15 monthly values in each time series, which is an amount of missing values corresponding to about 2 % of their total observations during the period 1955–2013. In these cases, a linear regression procedure was employed to complete or correct the temperature record, based on the recorded values in neighbouring highest correlated reference stations.

Prior to computing long-term trends, the homogeneity of temperature time series with respect to non-climatic influences must be assessed. In the present study, seasonal and annual temperature data series were tested for discontinuities using two homogeneity tests: the Alexanderson test (Alexanderson

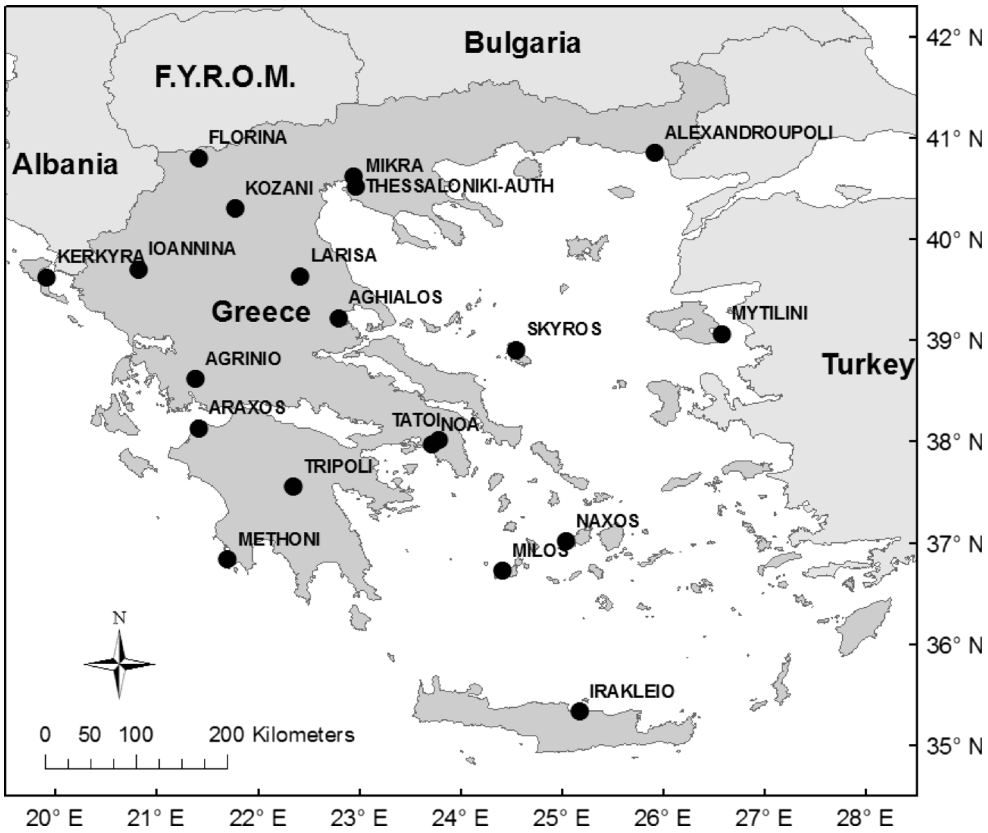

Fig. 1 The geographical distribution of the 20 stations used in the study

Table 1 Geographical coordinates and altitudes of the 20 stations used in this study

Station		Latitude	Longitude	Altitude (m)
1.	Aghialos	39° 13′N	22° 48′E	15
2.	Agrinio	38° 37′N	21° 25′E	46
3.	Alexandroupoli	40° 51′N	25° 57′E	4
4.	Araxos	38° 10′N	21° 25′E	14
5.	Florina	40° 48′N	21° 25′E	662
6.	Ioannina	39° 40′N	20° 51′E	484
7.	Iraklio	35° 20′N	25° 11′E	48
8.	Kerkyra	39° 37′N	19° 55′E	2
9.	Kozani	40° 20′N	21° 48′E	625
10.	Larisa	39° 38′N	22° 25′E	73
11.	Methoni	36° 50′N	21° 43′E	34
12.	Milos	36° 43′N	24° 25′E	182
13.	Mytilene	39° 04′N	26° 35′E	5
14.	Nat. Obs. Athens	37° 58′N	23° 43′E	107
15.	Naxos	37° 06′N	25° 24′E	9
16.	Skyros	38° 54′N	24° 33′E	4
17.	Tatoi	38° 06′N	23° 47′E	235
18.	Thessaloniki-AUTH	40° 37′N	22° 57′E	31
19.	Thessaloniki-Mikra	40° 31′N	22° 58′E	5
20.	Tripoli	37° 33′N	22° 21′E	663

1986) and the cumulative residuals test (Allen et al. 1998). Both methods compare data series to a reference series, which is a standard methodology of detecting non-climatic inhomogeneities.

Alexanderson test assumes that a standardized difference or ratio series between the reference data and the data that are being assessed is fairly constant. It sequentially segments the series into two parts and then compares the mean for each of the two segments before and after the point of segmentation to estimate a sequence of the test statistic T_i ($1 \le i \le n$, where N is the size of the time series). The $T_o = \max(T_i)$ indicates the year which is the most probable for a break. The critical value of T_o at the 95 % significance level, for $n = 59$, is 8.71.

The cumulative residuals homogeneity test assumes that a time series is homogeneous if its cumulative residuals from a regression line based on the reference data set are not biased. The bias hypothesis is tested for a given significance level by testing graphically whether the cumulative residuals E_i can be contained within an ellipsis. The magnitude of the ellipsis depends on the size of the time series, on the standard deviation of the data series being tested and on the significance level used to test the hypothesis. In the present study, this procedure was automated by computing the statistic ΔE_o as the maximum (minimum) distance of the cumulative residuals E_i from the ellipse when E_i is not contained (contained) within the ellipsis. A positive ΔE_o indicates an inhomogeneity in the time series.

Both methods compare data series to a reference series from either an individual station or a composite series form the closest stations. Using as a reference series only data from an individual station can be problematic because any detected discontinuity (or absence of discontinuity) may be caused (or masked) by climatic influences (Peterson et al. 1998). To isolate better the non-climatic influences, data from a number of nearby stations can be used as an indicator of the regional climate.

In the present study, to minimize potential inhomogeneities in the reference series, a composite reference series was built for each of the 20 stations, as a simple average of a number of 3 to 5 highly correlated neighbouring stations. Only stations which were strongly correlated with the candidate station (correlation over 0.8), at 95 % significance level, were used in the development of the composite reference series. After the homogeneity test was applied on all the stations, those series with inhomogeneities were removed from the composite series and new reference series were created as before.

Statistics of two homogeneity tests (T_o for Alexanderson test and ΔE_o for cumulative residuals test) for annual, winter and summer time series of the 20 stations used in this study are presented in Table 2. Both tests have found statistically significant inhomogeneities in two stations (Kerkyra and Skyros), for annual and seasonal data series (with the exception of summer). These two stations were excluded from further analysis.

Finally, the anomalies of seasonal and annual mean temperatures as departures from the mean of the 1961–1990 period were estimated for each station. Annual and winter temperature was conventionally computed to correspond to the period started from December of the previous year.

The respective temperature time series for the Northern Hemisphere (NH) expressed as anomalies from the average of the 1961–1990 period were also used in this study to compare with time series over Greece. This dataset (CRUTEM4) has been developed by the Climatic Research Unit of the University of East Anglia in conjunction with the Hadley Centre at the United Kingtom Met Office and comprises land air temperature anomalies on a 5° × 5° grid (Jones et al. 2012).

2.2 Satellite temperature data

Temperature data of the lower troposphere (0–8 km) derived by the Microwave Sounding Unit (MSU) operating on NOAA polar-orbiting platforms were also used in this study. MSU is a microwave atmospheric sounder making measurements of microwave radiation emitted by the atmosphere in four channels ranging from 50.3 to 57.95 GHz on the oxygen absorption band, with a 115-km horizontal spatial resolution, from late 1978 to the early 2000s. These four channels measure temperature through clouds from the surface to the lower stratosphere. The follow-on instrument Advanced Microwave Sounding Unit (AMSU) began operation in 1998. It makes measurements using a greater number of channels, with larger spatial resolution. Using the channels that most closely match the four channels of the MSU instruments, the MSU-based datasets can be extended up to the present.

The data were adjusted for time-dependent biases by NASA and the Global Hydrology and Climate Center (GHCC) at the University of Alabama in Huntsville (UAH) and comprise low-troposphere, mid-troposphere and lower stratosphere monthly mean temperature anomalies (departures from the average of the 1980–2010 base period). Given that the satellite sensors deteriorate over time, the data need to be corrected for satellite drift and orbital decay, diurnal adjustment, etc. After being corrected, the UAH lower troposphere temperature data match more closely with temperature from radiosondes and other sources of satellite data such as the Remote Sensing Systems (RSS) temperature data (Christy et al. 2007).

For the present study, the UAH lower troposphere seasonal and annual temperature anomalies for NH and the area of Greece (20–28°E and 34–42°N) for the period 1979–2013 were used to compare lower troposphere with surface air temperature trends.

2.3 Statistical tests for trend analysis

Possible trends in the time series are detected by applying the three tests proposed in the study of Feidas et al. (2004):

i. *The first test* is a simple linear regression model based on the linear equation $Y_t = a^{\wedge} + b^{\wedge} t + E_t$, where t is time (in years) Y_t, is temperature in year t, $b^{\wedge}$ is the slope of the trend line and E_t is the residual. Under the usual assumption that the residuals E_t are independent and normally distributed, the null hypothesis H_o: $b = 0$ is true when the ratio $t_1 = b^{\wedge} / s_1{}^{\wedge}(b^{\wedge})$ is distributed as Student's t with n-2 degrees of freedom, where $s_1{}^{\wedge}(b^{\wedge})$ is the estimated standard error of slope $b^{\wedge}$. The null hypothesis is rejected with a two-tailed t-test when the test statistic t_1 is greater than the critical value $t_{n-2;a/2}$, where a is the significance level.
ii. *The second test* is a variation of the linear regression-based model with the rigorous assumption that residuals E_t are not independent neither normally distributed. In this case, it is assumed that there is autocorrelation among the residuals that must be taken into account in the estimation of the standard error $s_2{}^{\wedge}(b^{\wedge})$ of slope $b^{\wedge}$ (Grenander 1954; Gryer 1986; Bloomfield and Nychka 1992). Again, the null hypothesis H_o is rejected by comparing the test statistic $t_2 = b^{\wedge} / s_2{}^{\wedge}(b^{\wedge})$ with the critical value $t_{n-2;a/2}$.

Table 2 Sift years and statistics of two homogeneity tests (T_o for Alexanderson test and ΔE_o for cumulative residuals test) for annual, winter and summer time series of the 20 stations used in this study. Positive ΔE_o and T_o greater than 8.71 indicate an inhomogeneity in the time series. Statistical significant inhomogeneities are indicated in *italics*

		Annual		Winter		Summer	
	Station	T_o	ΔE_o	T_o	ΔE_o	T_o	ΔE_o
1.	Aghialos	8.3	−0.02	3.1	−0.39	6.5	−0.08
2.	Agrinio	6.7	−0.04	8.1	−0.31	8.7	0.0
3.	Alexandroupoli	6.6	−0.36	5.4	−0.06	6.2	−0.03
4.	Araxos	4.1	−0.19	4.5	0.0	7.8	−0.05
5.	Florina	3.8	−0.50	5.9	−0.68	3.0	−0.10
6.	Ioannina	7.4	−0.13	5.6	−0.75	5.2	−0.73
7.	Iraklio	6.9	−0.14	3.5	−0.40	7.0	−0.67
8.	Kerkyra	*24.3 (1978)*	*+2.41 (1978)*	*23.2 (1974)*	*+1.56 (1975)*	7.4	−0.31
9.	Kozani	7.4	−0.24	3.9	0.0	7.5	−0.57
10.	Larisa	4.9	−0.14	3.4	−0.72	8.1	−0.23
11.	Methoni	5.1	−0.26	6.4	−0.18	5.3	−0.33
12.	Milos	5.1	−0.15	5.2	−0.01	6.8	−0.28
13.	Mytilene	3.8	−0.03	5.6	−0.02	5.9	−0.05
14.	Nat. Obs. Athens	6.9	−0.06	6.4	−0.17	8.7	−0.45
15.	Naxos	8.0	−0.15	6.3	−0.53	7.7	−0.15
16.	Skyros	*40.3 (1992)*	*+2.13 (1980)*	*23.5 (1981)*	*+3.48 (1981)*	*16.0 (1992)*	−0.31
17.	Tatoi	3.3	−0.51	8.1	−0.18	5.7	−0.42
18.	Thessaloniki-AUTH	8.6	−0.09	8.6	0.00	5.4	−0.22
19.	Thessaloniki-Mikra	5.7	−0.09	7.0	−0.52	6.0	−0.03
20.	Tripoli	6.1	−0.84	6.8	−0.60	8.0	−0.27

iii. *The third test* implemented is the Mann-Kendall non-parametric rank statistic test (Sneyers 1990). First, the statistical test d_i is calculated by the sum of the number m_i of terms Υ_j in the series preceding each term Υ_i ($i > j$), such that $\Upsilon_j < \Upsilon_i$:

$$d_i = \sum_i m_i \tag{1}$$

Then, the test computes the statistics $u(d_i)$ for each term i of the time series ($1 \le i \le n$), with the following formula (Michell et al. 1966):

$$u(d_i) = [d_i - E(d_i)]/\sqrt{\mathrm{var}(d_i)} \tag{2}$$

where $E(d_i)$ and $\mathrm{var}(d_i)$ are the mean and variance, respectively, of the d_i distribution:

$$E(d_i) = i(i-1)/4, \mathrm{var}(d_i) = i(i-1)(2i+5)/72 \tag{3}$$

The null hypothesis H_o: $b = 0$ is rejected when the last value $u(d_n)$ of the $u(d_i)$ statistics for the final nth term of the series is greater–in absolute value–than 1.96 for a two-tailed test at 95 % level of significance.

The Mann-Kendall test is deemed the most suitable for the trend analysis of climatological time series (Goosens and Berger 1986). The advantage of the Mann-Kendall rank statistic is that it enables a climatic discontinuity (the start of an abrupt and permanent change) to be localized approximately. To this end, the retrograde series $u'(d_i)$ is calculated using the same methodology applied for the $u(d_i)$ statistic. The beginning of the change is localized based on the graphical representation of the $u(d_i)$ and $u'(d_i)$ series, $1 \le i \le n$, denoted as C_1 and C_2, respectively. An significant increasing (decreasing) trend is identified at 95 % level of significance when the increasing (decreasing) values of the $u(d_i)$ become greater than the critical value 1.96. The intersection of the curves C_1 and C_2 identifies the start of the trend or change, whereas the frequent overlap of these curves denotes the absence of any trend in the time series.

2.4 Pressure indices

One of the objectives of this study is to relate the variability of air temperature in Greece with regional and large-scale atmospheric circulation. To this end, we used the three circulation indices (NAOI, MOI and MCI) of the study of Feidas et al. (2004) along

Table 3 Values of the slope b (in °C/year) of the trend line and of the three statistics t_1, t_2 and $u(d_n)$ for the annual and seasonal temperature observations of the 18 homogeneous stations in Greece (1955–2013) (*Italicized values* indicate a 95 % level of significance)

Station	Winter				Spring				Summer				Autumn				Annual			
	b	t_1	t_2	$u(d_n)$	b	t_1	t_2	$u(d_n)$	b	t_1	t_2	$u(d_n)$	b	t_1	t_2	$u(d_n)$	b	t_1	t_2	$u(d_n)$
Aghialos	0.009	1.25	2.18	0.99	*0.020*	*2.81*	*2.80*	*2.89*	*0.027*	*4.90*	*2.88*	*4.30*	0.009	1.31	1.73	1.08	*0.016*	*4.09*	*2.81*	*3.39*
Agrinio	−0.013	−1.92	−1.53	−1.72	0.010	1.62	1.24	1.50	0.014	2.00	0.84	1.50	−0.007	−1.19	−1.01	−1.34	0.000	−0.06	−0.03	−0.05
Alexandroupoli	−0.007	−0.75	−0.84	−0.53	*0.025*	*3.69*	*3.74*	*3.46*	*0.039*	*5.87*	*2.71*	*4.65*	0.006	0.75	0.61	0.61	*0.016*	*3.28*	1.74	*2.70*
Araxos	*−0.012*	*−2.01*	−1.79	*−1.98*	*0.012*	*2.18*	1.69	*2.30*	*0.024*	*4.20*	*2.10*	*3.68*	−0.002	−0.28	−0.20	−0.27	0.006	1.54	0.70	1.58
Florina	−0.012	−0.97	−1.03	−0.71	0.004	0.52	0.69	0.90	*0.022*	*2.75*	1.77	*2.14*	0.003	0.27	0.22	0.20	0.004	0.77	0.43	0.23
Ioannina	−0.010	−1.45	−1.50	−1.24	0.007	1.12	1.08	1.22	0.019	2.28	1.64	1.71	−0.008	−1.17	−1.15	−1.42	0.002	0.49	0.27	0.09
Iraklio	−0.006	−1.08	−0.85	−1.31	0.004	0.79	0.64	0.52	*0.013*	*2.96*	1.38	*2.74*	0.011	1.94	1.50	1.59	0.006	1.53	0.75	1.20
Kozani	0.000	−0.02	−0.02	0.16	*0.026*	*3.07*	*3.25*	*3.00*	*0.037*	*4.32*	*2.90*	*3.71*	0.008	0.98	1.07	0.73	*0.018*	*3.52*	*2.17*	*3.00*
Larisa	−0.006	−0.72	−0.73	−0.49	*0.015*	*2.15*	*2.56*	*2.05*	0.014	1.96	1.15	1.62	0.003	0.49	0.41	0.18	0.007	1.48	0.84	1.03
Methoni	−0.010	−1.75	−1.45	−1.75	0.005	1.08	0.75	1.33	*0.015*	*3.21*	1.84	*2.90*	−0.001	−0.18	−0.14	−0.48	0.003	0.79	0.38	0.46
Milos	−0.005	−0.83	−0.60	−0.86	*0.017*	*2.66*	1.90	*2.27*	*0.041*	*7.25*	*3.08*	*5.15*	*0.017*	*2.47*	1.59	*2.11*	*0.017*	*3.81*	1.71	*3.04*
Mytilene	−0.008	−0.97	−0.75	−0.74	*0.020*	*3.00*	*2.71*	*2.78*	*0.041*	*7.02*	*2.89*	*4.85*	0.011	1.64	1.17	1.42	*0.016*	*3.41*	1.59	*2.86*
Nat. Obs. Athens	−0.009	−1.34	−1.90	−1.29	*0.017*	*2.62*	*3.56*	*2.54*	*0.030*	*5.13*	*2.71*	*4.15*	0.004	0.57	0.79	0.40	*0.010*	*2.64*	1.87	*2.28*
Naxos	−0.003	−0.50	−0.49	−0.54	*0.011*	*2.14*	*2.47*	1.80	*0.027*	*6.12*	*3.51*	*4.92*	*0.016*	*2.62*	*2.47*	*1.98*	*0.013*	*3.57*	*2.22*	*3.18*
Tatoi	−0.009	−1.19	−1.10	−1.42	*0.014*	*2.00*	1.74	*2.05*	*0.026*	*4.23*	*2.75*	*3.54*	0.004	0.56	0.50	0.21	0.009	1.97	1.16	1.46
Thessaloniki-AUTH	0.004	0.49	0.47	0.53	0.013	1.95	1.63	1.85	*0.024*	*3.98*	1.72	*3.09*	0.004	0.47	0.31	−0.02	0.011	2.43	1.11	1.65
Thessaloniki-Mikra	0.008	1.08	1.38	1.31	*0.017*	*2.65*	*2.32*	*2.47*	*0.022*	*3.65*	1.63	*3.21*	*0.017*	*2.27*	1.92	*2.06*	*0.016*	*3.74*	1.91	*3.29*
Tripoli	−0.007	−1.04	−1.30	−0.87	*0.021*	*3.01*	*4.06*	*2.66*	*0.018*	*2.65*	1.69	*2.40*	0.004	0.63	0.75	0.09	0.009	2.17	1.51	1.79

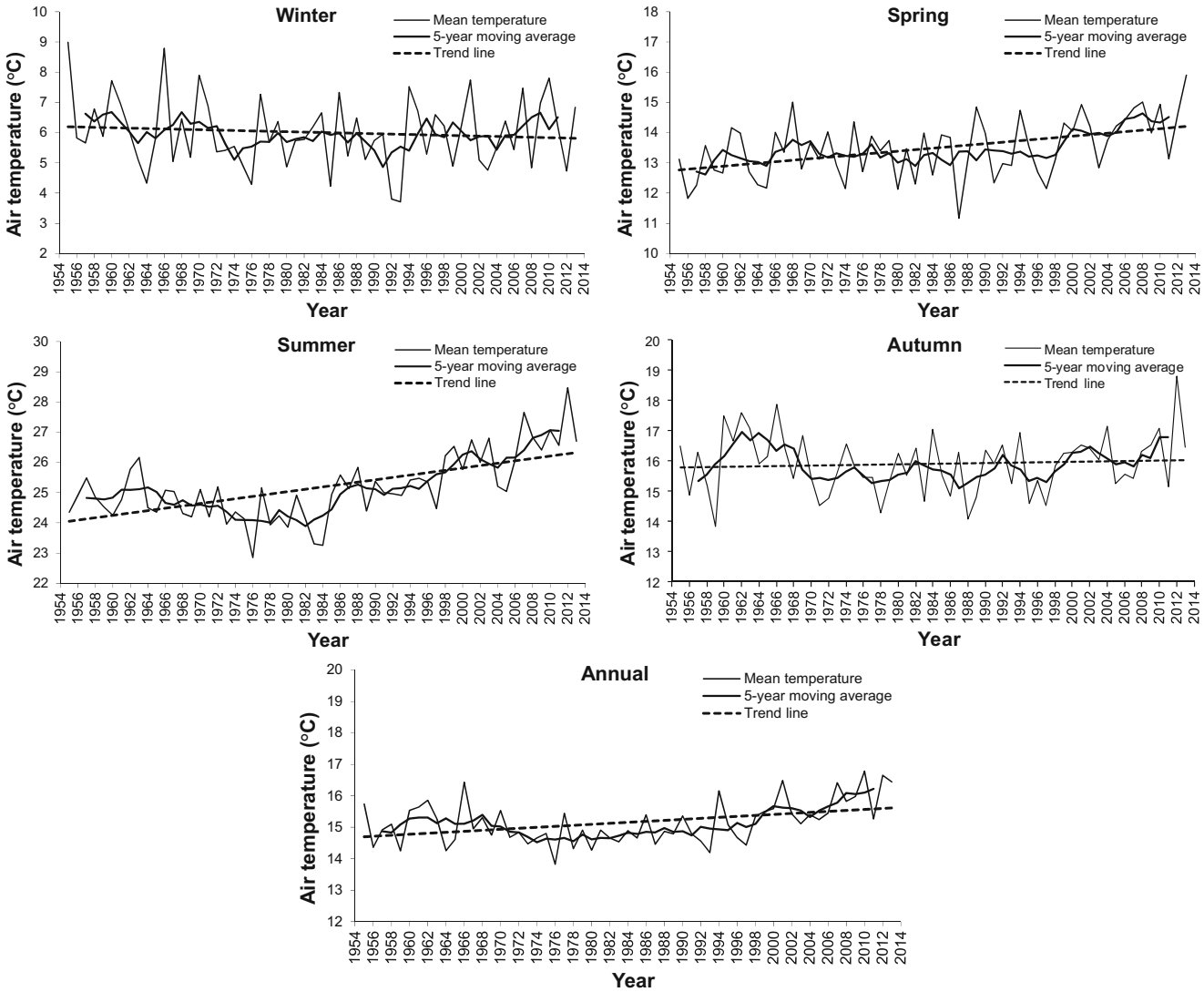

Fig. 2 Graphs of observed values, 5-year moving average and trend line of seasonal and annual air temperature time series at the station of Alexandroupoli for the period 1955–2013

with another two new ones (NCPI and EMPI) which were found to interpret better the regional surface air temperature variability in the Eastern Mediterranean.

a. *NAOI.* The North Atlantic Oscillation (NAO) is considered the dominant large-scale pattern of climate variability in the North Atlantic atmospheric circulation. It is a large-scale seesaw in atmospheric pressure between the subtropical Azores high and the subpolar Icelandic low pressure system. Opposite NAO states are associated with opposite climate fluctuations between western Greenland/Mediterranean and northern Europe/Scandinavia (Walker 1924; Walker and Bliss 1932; van Loon and Rogers 1978; Rogers and van Loon 1979). The positive phase of NAO reflects a simultaneous strengthening of the two NAO centres of action which is usually associated with stronger than average westerlies over the middle latitudes leading to colder, dryer weather conditions over Greenland/Mediterranean and a warmer, wetter weather conditions over northern Europe/Scandinavia. Analogously, the negative phase of NAO corresponds to a simultaneous weakening of the two NAO centres which is linked with a reverse climate pattern. Although the NAO is present for all seasons, it is most dominant during winter due to an intensified sea-air temperature contrast (Barnston and Livezey 1987).

The NAO index (NAOI) is based on the difference of normalized mean sea level pressure (SLP) between stations representative of the dipole centres (Azores high and Icelandic low). In this study, seasonal and annual NAO indices provided by National Center of Atmospheric Research (NCAR) were used (https://climatedataguide.ucar.edu/climate-data/hurrell-north-atlantic-oscillation-nao-index-station-based). These indices were defined based on

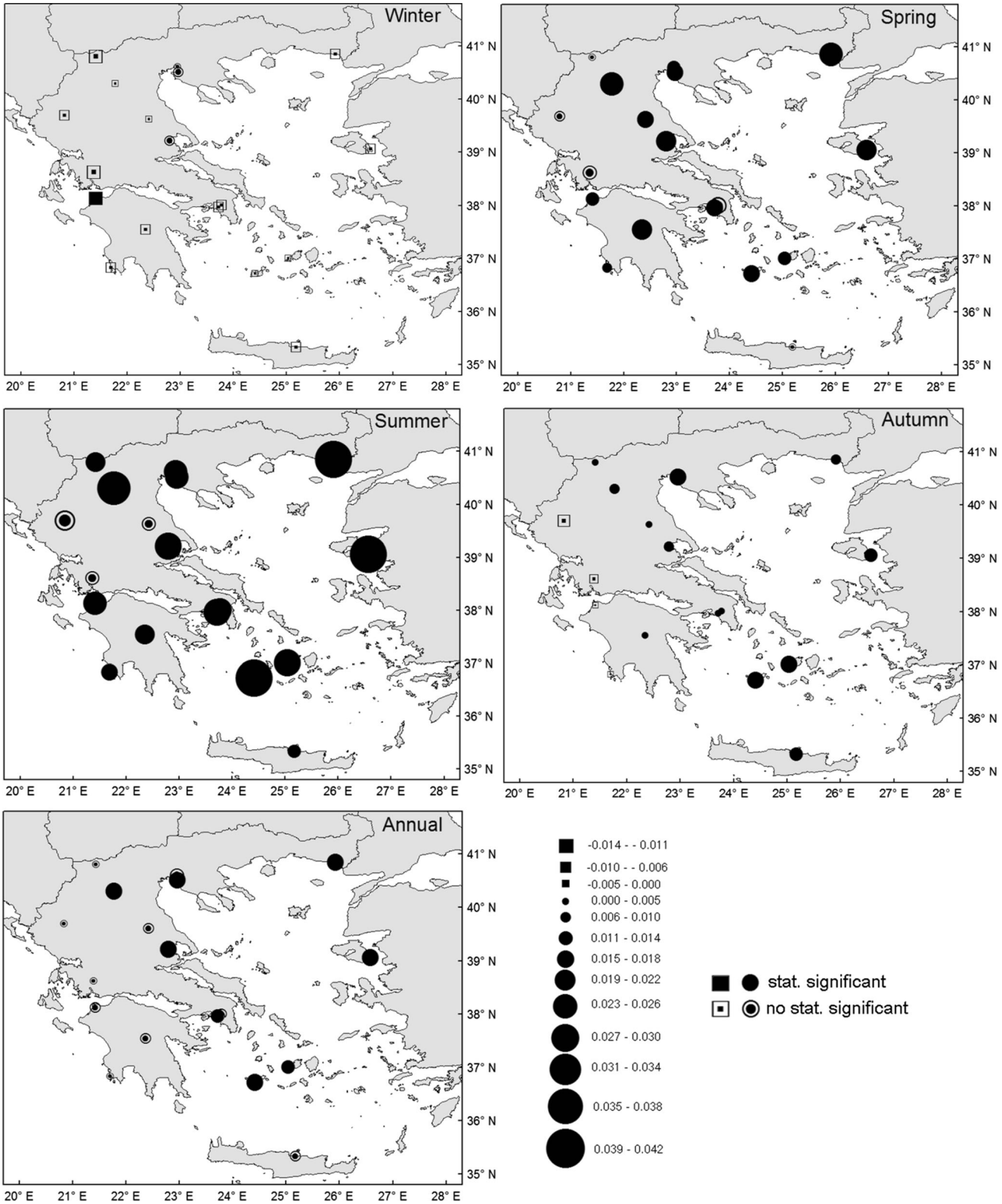

Fig. 3 Maps with the spatial distribution of the seasonal and annual air temperature trend (in °C/year) of the time series (1955–2013). *Circles* and *squares* denote positive and negative values, respectively. The *filled black symbols* denote a 95 % significance level

the locations of Lisbon (Portugal) and Reykjavik (Iceland) and are an update of the data published in Hurrell (1995).

b. *MOI.* The 'Mediterranean Oscillation' (MO) is a dipole pressure pattern with opposite upper level pressure

Table 4 Same as Table 3 but for temperature time series spatially averaged over Greece and the Northern Hemisphere (*Italicized values* indicate a 95 % level of significance)

	Winter				Spring				Summer				Autumn				Annual			
	b	t_1	t_2	$u(d_n)$	*b*	t_1	t_2	$u(d_n)$	*b*	t_1	t_2	$u(d_n)$	*b*	t_1	t_2	$u(d_n)$	*b*	t_1	t_2	$u(d_n)$
Greece	−0.006	−0.85	−0.80	−0.78	*0.013*	*2.28*	*2.01*	*2.14*	*0.025*	*4.56*	*2.19*	*3.84*	0.005	0.86	0.70	0.63	*0.010*	*2.47*	1.23	*2.06*
NH	*0.023*	*7.82*	*5.94*	*6.09*	*0.026*	*13.8*	*10.9*	*7.68*	*0.021*	*12.5*	*6.00*	*7.17*	*0.022*	*10.1*	*5.04*	*6.66*	*0.024*	*13.6*	*7.00*	*7.49*

between the western and eastern Mediterranean basin (Conte et al. 1989; Colacino and Conte 1993; Piervitali et al. 1999; Kutiel et al. 1996; Douguedroit 1998; Maheras et al. 1999; Maheras and Kutiel 1999; Criado-Aldeanueva and Soto-Navarro 2013). The MO phases are linked to the cyclogenesis activity in the Mediterranean with positive phase induced by anomalously intense cyclogenesis and vice versa (Sušelj and Bergant 2006). Conte et al. (1989) proposed an index to measure the intensity of MO expressed as the difference of normalized geopotential height anomalies at the 500 hPa surface at Algiers (western basin) and Cairo (eastern basin).

The Mediterranean Oscillation Index (MOI) was calculated in this study using the monthly 2.5° × 2.5° gridded reanalysis data of the National Center for Environmental Prediction (NCEP) and NCAR (Kalnay et al. 1996) provided by the Earth System Research Laboratory (ESRL), Physical Science Division of NOAA, from their website at http://www.esrl.noaa.gov/psd/, since the available recorded time series in Cairo and Algiers stations were not complete. Moreover, gridded values have the advantage of being less sensitive to errors in single station records.

c. *MCI.* The Mediterranean Circulation Index (MCI) is a new index devised by Brunetti et al. (2002), aiming to develop an index more suitable for the central Mediterranean based on opposite sea level pressure pattern between the northwestern and south-eastern Mediterranean. It is expressed as the normalized SLP difference between Marseille and Jerusalem. In this study, MCI was calculated using the Trenberth Northern Hemisphere monthly SLP gridded values calculated on a 5° (72 × 15) latitude × longitude grid from NCAR. Data were extracted using the Climate Explorer of the Royal Netherlands Meteorological Institute (KNMI) (http://climexp.knmi.nl).

d. *EMPI.* The Eastern Mediterranean Pattern (EMP) is a teleconnection pattern of the upper atmospheric circulation at 500 and 300 hPa between the eastern Mediterranean Sea and northeastern Atlantic, appearing mainly in winter (Hatzaki et al. 2007). This dipolar oscillation pattern is also present in autumn but is significantly weakened with its position being shifted eastwards (Hatzaki et al. 2007).

The EMP index (EMPI) was defined by Hatzaki et al. (2007) as follows:

$$X_i = \mathrm{gpm}(25°\mathrm{W}, 52.5°\mathrm{N}) - \mathrm{gpm}(22.5°\mathrm{E}, 32.5°\mathrm{N}) \quad (4)$$

where i indicates the time step, and gpm (geopotential metres) is the mean monthly or seasonal geopotential height at the 500 hPa of the grid point representing the centre of each pole.

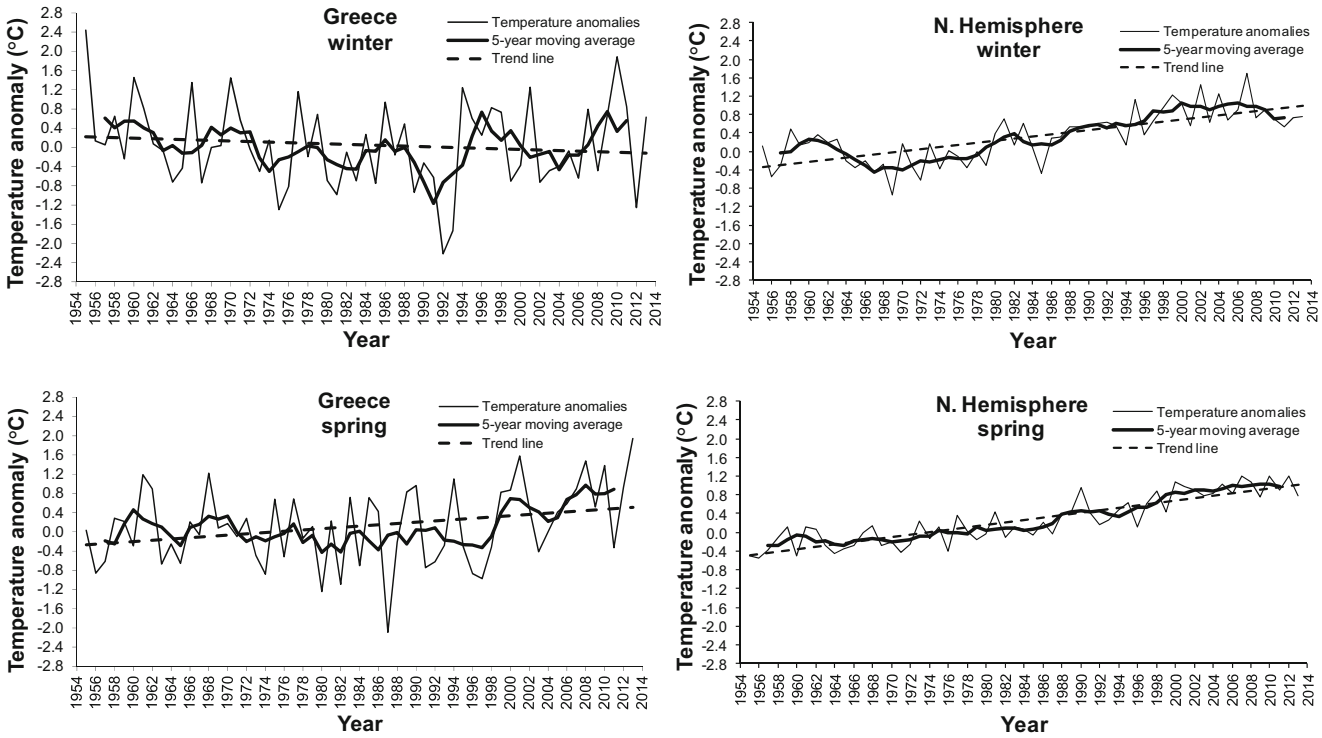

Fig. 4 Graphs of observed values, 5-year moving average and trend line of seasonal and annual air temperature anomalies (relative to 1960–1990 average) in Greece and Northern Hemisphere for the period 1955–2013

The EMPI is then calculated as the standardized difference between the index (X) defined in equation (4) and its seasonal long-term average ($\overline{X}$):

$$\mathrm{EMPI}_i = \frac{X_i - \overline{X}}{\sigma} \tag{5}$$

where σ is the standard deviation of X. In this study, the EMPI was calculated using the monthly 2.5° × 2.5° gridded reanalysis data of NCEP/NCAR.

A negative phase of the EMP is associated with an increased zonal flow over Europe. On the contrary, during the positive EMP phase, the Atlantic anticyclone is strengthened inducing an intensified northerly meridional flow toward the central Mediterranean.

e. *NCPI.* The North Sea Caspian Pattern (NCP) is an upper level teleconnection between the North Sea and the North Caspian centres of action. It was defined by Kutiel and Benaroch (2002) who applied a Geographic Information Systems technique along with a linear correlation between pressure grid points to define these centres of action.

The NCP has been found to satisfactorily interpret the regional climate variability in the Eastern Mediterranean, with regard to both the precipitation and the surface air temperature (Brunetti and Kutiel 2011; Nastos et al. 2011; Kutiel and Brunetti 2010; Hatzaki et al. 2007; Kutiel and Türkeş 2005; Kutiel and Benaroch 2002; Kutiel et al. 2002). Although the NCP is more pronounced during winter, it is also prominent during the transitional seasons (Kutiel and Benaroch 2002).

A negative (positive) NCP phase indicates an increased counter-clockwise (clockwise) anomaly circulation around the North Sea pole of the NCP and an increased clockwise (counter-clockwise) anomaly circulation anomaly around the North Caspian pole of the NCP (Kutiel and Benaroch 2002). This pattern induces an enhanced south-westerly (northeasterly) air flow towards the Balkan Peninsula and western Turkey.

An index expressing the NCP intensity was proposed by Kutiel and Benaroch (2002) as the normalized difference of 500 hPa geopotential height between averages of North Sea (0°E, 55°N and 10°E, 55°N) and North Caspian (50°E, 45°N and 60°E, 45°N) poles. In this study, the NCP index is calculated for each month of period 1955–2013 according to the modified formula proposed by Brunetti and Kutiel (2011), in which each of the two poles is formed by five grid points at a 2.5° × 2.5° resolution instead of 10° × 10°:

$$X_i = \overline{\mathrm{gpm}}\,(0°, 2.5°, 5°, 7.5°, 10°\mathrm{E}; 55°\mathrm{N}) - \overline{\mathrm{gpm}}\,(50°, 52.5°, 55°, 57.5°, 60°\mathrm{E}; 45°\mathrm{N}) \tag{6}$$

where i denotes the time step and $\overline{\mathrm{gpm}}$ (geopotential metres) is the average geopotential height of the five

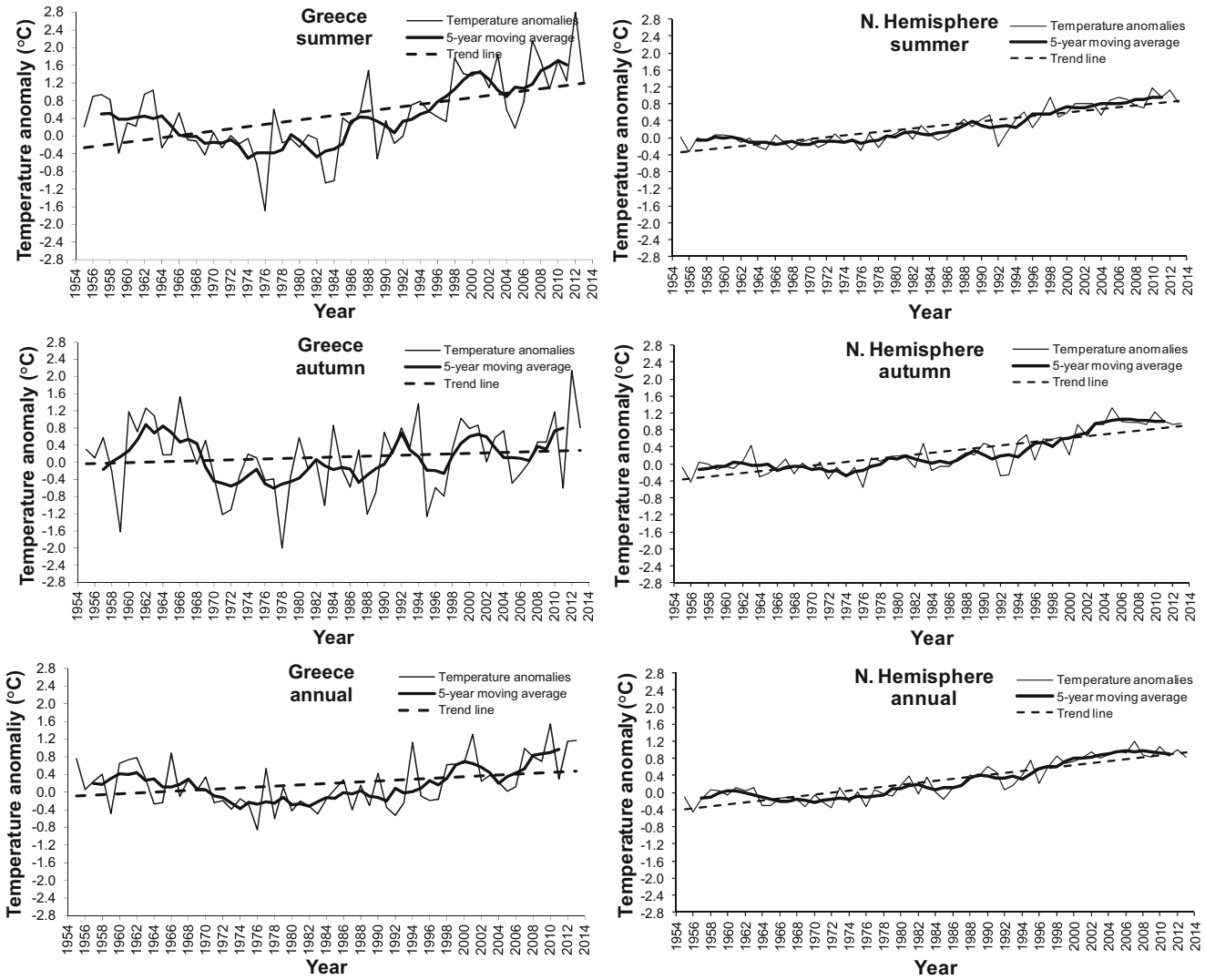

Fig. 4 (continued)

grid points, forming each of the two centres of actions, respectively.

For each month and season, these values were then standardized as follows:

$$\mathrm{NCPI}_i = \frac{X_i - \overline{X}}{\sigma} \tag{7}$$

where $\overline{X}$ is the monthly long-term average of X_i and σ is its standard deviation.

The NCPI was calculated using the monthly 2.5° × 2.5° gridded reanalysis data of NCEP/NCAR.

2.5 Pressure and temperature gridded data

Seasonal mean gridded sea-level pressure, 500 hPa geopotential height and surface air temperature data on a 2.5° latitude × 2.5° longitude grid were used to construct maps and compare the pressure and temperature pattern over Europe as composite anomalies from the mean of the period 1955–2013 for selected extreme positive and negative values of the pressure indices. This grid was computed by the NCEP/NCAR reanalysis monthly means (Kalnay et al. 1996). The same temperature dataset was used to depict the spatial distribution of correlation between the winter air temperature and circulation indices over Europe.

3 Results

3.1 Trends in surface temperature observations

Temperature trends in surface observations were detected by applying not only one but three statistical tests to the annual and seasonal temperature records of the 18 Greek weather

Table 5 Approximate starting year of an abrupt temperature change according to the progressive and retrograde Mann-Kendall $u(d_i)$ and $u'(d_i)$ statistics for the annual and seasonal air temperature observations of the 18 stations in Greece (1955–2013)

Station	Winter	Spring	Summer	Autumn	Annual
Aghialos	*	2004+	1997+	1963- (1998+)	2005+
Agrinio	1963-	*	2010+	1969-	1956-
Alexandroupoli	*	2004+	2000+	*	2006+
Araxos	1963-	2005+	2006+	1964-(2012+)	1962- (2009+)
Florina	1961-(2007+)	*	1956- (2007+)	1964- (2008+)	1961- (2007+)
Ioannina	1962- (2010+)	*	1957- (2011+)	1968-	1962- (2012+)
Iraklio	1964- (2010+)	1963- (2013+)	2003+	*	*
Kozani	*	2005+	1995+	1968- (2012+)	2000+
Larisa	1956- (2009+)	2005+	1958- (2010+)	1964- (2012+)	2012+
Methoni	1967-	1963- (2009+)	1998+	1964- (2012+)	1963- (2009+)
Milos	1956-(2010+)	2006+	1997+	2006+	2005+
Mytilene	1956- (2010+)	2004+	1997+	*	2006+
Nat. Obs. Athens	1956-	2005+	1995+	*	2005+
Naxos	1956- (2010+)	*	1997+	1997+	2006+
Tatoi	1967-	2007+	1997+	*	1962- (2008+)
Thessaloniki-AUTH	*	2007+	2006+	1968- (2012+)	2012+
Thessaloniki-Mikra	*	2005+	2005+	2008+	2005+
Tripoli	*	2004+	1998+	1964- (2012+)	*

*No abrupt temperature change at the 95 % level of significance

+Means a warming

-Means a cooling

( )Approximate year of a new change in a trend which is not statistically significant

stations for the period 1955–2013. Table 3 presents the slope b (in °C/year) of the linear trend, as found by the first linear regression test, and the values of the three statistics t_1, t_2 and $u(d_n)$ for the annual and seasonal time series. A trend line is deemed to be statistically significant when found out as such by at least two statistical tests (the first regression-based model and one of the other two tests). There are many stations with all three tests confirming a statistically significant trend. In the few cases in which only two out of the three tests result statistically significant trends, the test returning results that are not statistically significant is always the stringent second test. Most of the statistically significant trends are found in summer, followed by spring and annual time series. All trends are positive for seasonal and annual temperature time series with the exception of winter.

Plots of the seasonal and annual temperature time series, along with the 5-year moving average and the trend line are presented for Alexandroupoli station, as an indicative case (Fig. 2). Statistically significant positive trends were found for summer, spring and annual temperatures series for this station.

The spatial distribution of seasonal and annual temperature trends (in °C/year) for the 18 stations is shown in Fig. 3. The filled black symbols (cycles and squares) denote a 95 % significance level. Figure 3 along with Table 3 can be used to identify the warming or cooling trend of the stations and assess their spatial distribution. An overall warming trend manifests in the annual time series, with almost half of the stations–distributed mainly in the eastern Greece and the Aegean Sea–presenting significant trends. Summer time series shows a pronounced, strong warming trend which is statistically significant for the majority of the stations. Only three stations located in central and NW Greece were found not having statistically significant trends. A warming trend also dominates in the spring time series, with 12 out of the 18 stations–distributed mainly in the eastern Greece and the

Table 6 Same as Table 5 but for temperatures spatially averaged over Greece and the Northern Hemisphere

	Winter	Spring	Summer	Autumn	Annual
Greece	1956- (2010+)	2006+	1998+	1963- (2010+)	2007+
Northern Hemisphere	1989+	1988+	1994+	1996+	1993+

+ Means a warming

- Means a cooling

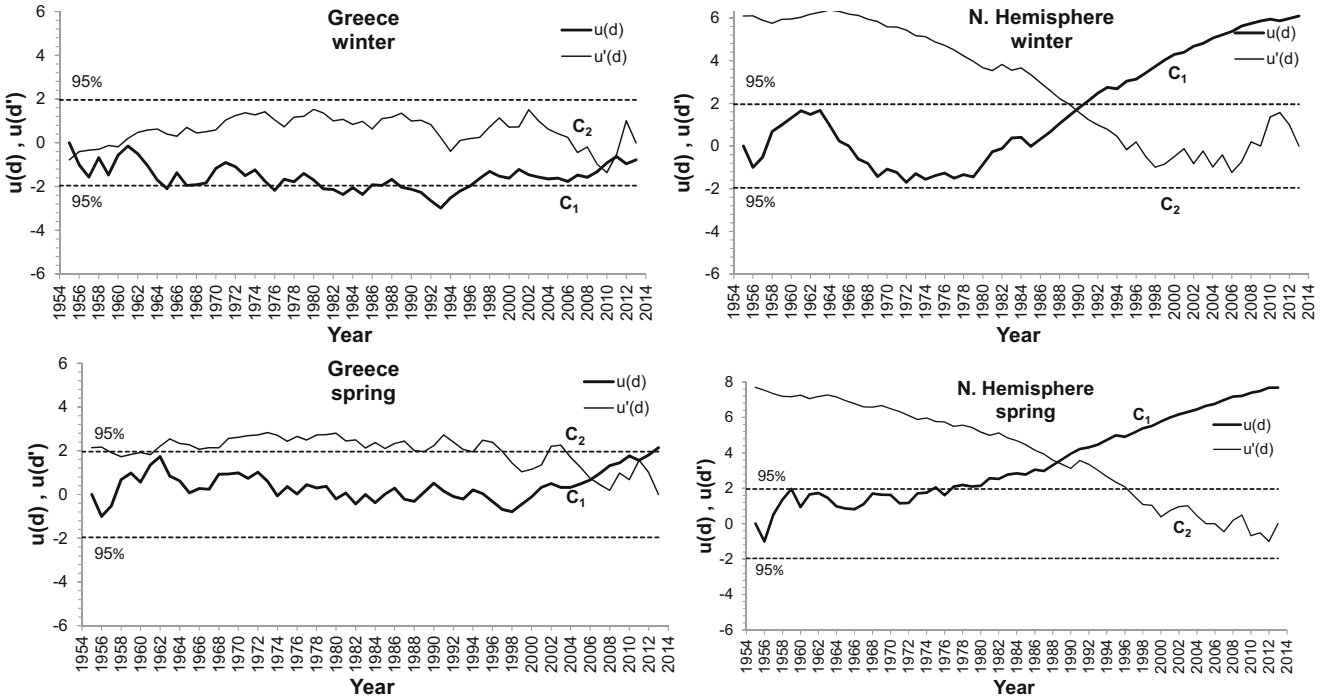

Fig. 5 Graphs of the progressive and retrograde Mann-Kendall $u(d_i)$ and $u'(d_i)$ statistics (indicated as C_1 and C_2), for seasonal and annual temperature anomalies averaged over Greece and Northern Hemisphere for the period 1955–2013

Aegean Sea–presenting significant trends (Table 3). Although autumn time series exhibit a warming trend for the majority of the stations, only three of them located in the Aegean Sea and Northern Greece present a statistically significant trend. A different picture emerges when examining the spatial distribution of the slope b for the winter time series, in which an overall cooling trend is manifested in the majority of the stations, being statistically significant in only one station.

It is interesting to investigate whether the previous results agree with the overall warming trend found at the hemispheric scale. For this reason, mean seasonal and annual temperature departures from the average of the 1961–1990 period were calculated for each station in Greece and averaged to estimate the Greek time series at the national scale. The results of the trend analysis for both Greece and NH are shown in Table 4 and plotted in Fig. 4.

Table 4 suggests that only summer, spring and annual temperature trends averaged over Greece exhibit an equivalent overall warming trend to that detected in the NH time series. Autumn temperature time series in Greece present a slight—though not statistically significant—warming trend, which, however, does not match the strong warming signal detected in the respective NH time series. Winter series in Greece exhibit a slight—again not statistically significant—cooling trend that is opposite to the strong warming trend found in the NH winter time series.

The temporal pattern of the time series for both areas, Greece and NH, has a common feature: the time series start with decreasing temperatures and after reaching a minimum, temperatures increase constantly up to the present (Fig. 4). This pattern is more distinct in the Greek time series. In general, the observed minimum lies around mid-1970s with the exception of winter in which the minimum for NH (late 1960s) and Greece (early 1990s) are not coincident. This means that winter temperature increase appears about 25 years later in Greece than in NH. This difference induced the overall slight cooling trend observed in the winter series of Greece during the entire period 1995–2013.

In general, it seems that the warming signal, detected in Greece only in summer in the study of Feidas et al. (2014) for the period 1955–2001, has now intensified and spread in other seasons. This warming appears to be mainly caused by the very high temperatures in the last decade (after 2004) of the record.

The graphical representation of the progressive and retrograde Mann-Kendall $u(d_i)$ and $u'(d_i)$ statistics of each time series was used to localize the intersection of the curves C_1 and C_2 and thus to identify the approximate starting year of an abrupt temperature change. This information is quoted in Table 5 for the full range of the mean annual and seasonal series. Each station is labelled with a year which identifies the beginning of a warming (+) or a cooling (−) trend. The second year in brackets denotes that a new change in a trend was found which, however, is not statistically significant. The asterisk signifies the absence of a climatic discontinuity for the entire period.

Table 5 suggests that annual series can be classified into two broad categories. The first category consists of stations

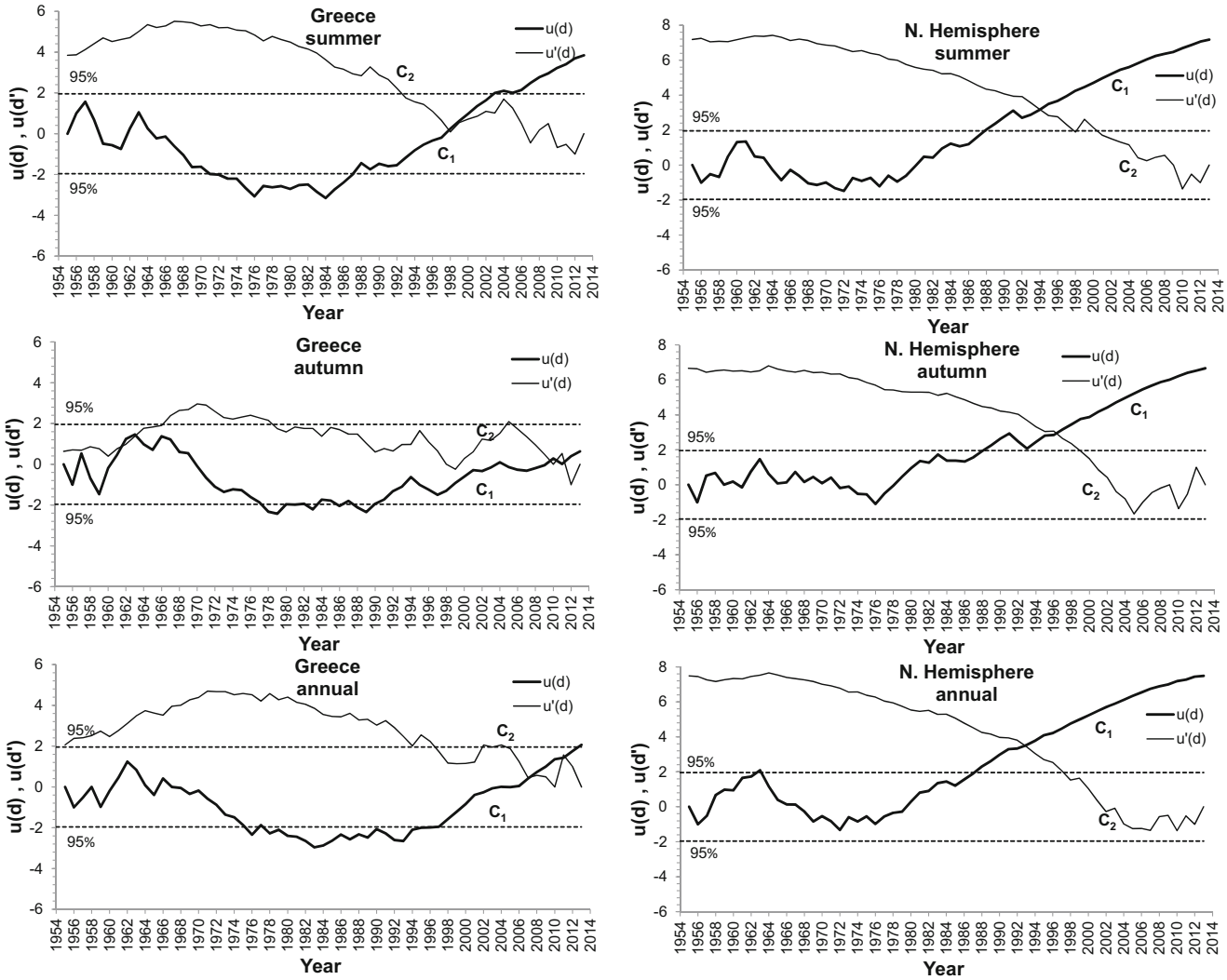

Fig. 5 (continued)

with a cooling trend starting around the early 1960s. This cooling trend seems to have been reversed recently, during the last 5 years of the period (2008–2013). The stations in the second category exhibit a net warming trend beginning during the 2000s. A cooling trend for winter and autumn time series began in many stations between late 1950s and mid 1960s, respectively; this trend, however, was reversed in most of these stations during the last years of the period (2008–2013). In contrast, most of the summer and spring series show a strong warming signal that started during the mid-1990s and 2000s, respectively. This late response of winter temperatures to global warming compared to the earlier and more intense summer temperature warming has been reported as well in other studies for eastern Mediterranean and Greece in particular (Nastos et al. 2011; Saaroni et al. 2003; Feidas et al. 2004).

Table 7 Values of the slope *b* (in °C/year) of the trend line for seasonal and annual time series of the satellite-derived (MSU) tropospheric temperatures and observed surface air temperature for Greece and the Northern Hemisphere for the period 1979–2013. (Italicized values indicate a 95 % level of significance)

	Winter	Spring	Summer	Autumn	Annual
(a) Satellite-derived					
Greece	*0.040*	*0.045*	*0.041*	*0.024*	*0.037*
Northern Hemisphere	*0.021*	*0.022*	*0.014*	*0.020*	*0.019*
(b) Surface observed					
Greece	0.019	*0.042*	*0.064*	*0.025*	*0.038*
Northern Hemisphere	*0.017*	*0.022*	*0.023*	*0.025*	*0.022*

'The results of the sequential Mann-Kendall analysis become clearer at the national scale (see Table 6 and Fig. 5). More precisely, winter and autumn series exhibit a cooling trend, beginning in 1956 and 1963, respectively, which, however, seems to start reversing recently (in 2010). A profound warming trend is evident in summer temperatures starting in 1998, while spring and annual series entered into a weaker warming trend one decade later (in 2006–2007).

Based on Table 6 and Fig. 5, the NH differentiates from Greece in showing a prominent, stable warming trend in all the seasonal and annual time series, which started between late 1980s and mid-1990s. Only summer temperatures in Greece follow this pattern. The other seasonal and annual time series in Greece have entered into a warm period more recently than in the NH.

3.2 Trends in satellite-derived temperature data

The same trend analysis was implemented to the satellite-derived (MSU) air temperature time series of the lower troposphere for the period 1979–2013. Table 7 (a) presents the slope *b* (in °C/year) of the linear trend line for seasonal and annual time series for Greece and NH. The graphs of the respective temperature time series and the trend line are provided in Fig. 6.

Table 7 (a) points out a statistically significant warming trend in tropospheric temperatures for both areas. Warming trend over Greece is, however, more pronounced than over the NH (0.24–0.45 °C per decade against 0.14–0.22 °C per decade). According to the sequential Mann-Kendall analysis, this warming trend started in mid-1990s for both areas.

The comparison of the satellite and surface temperature trends for the same period (1979–2013) (see Table 7 (a), (b)) shows, in general, a very good agreement for both Greece and NH, with the exception of winter and summer for Greece. More precisely, satellite-induced temperatures of the lower troposphere for Greece show a warming trend, which is significantly higher for winter and lower for summer than that for the surface records.

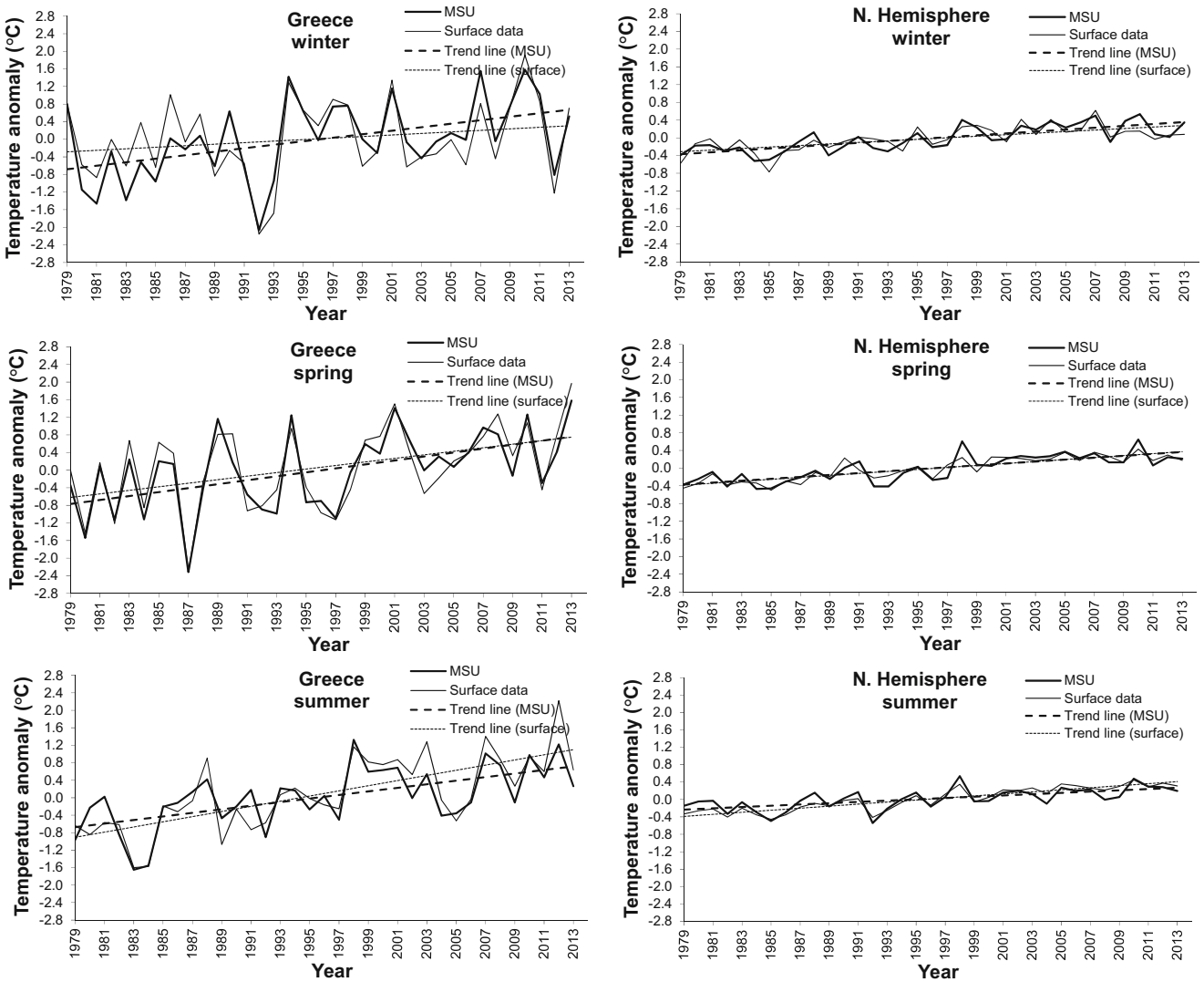

Fig. 6 Graphs of satellite-derived (MSU) tropospheric temperature anomalies and surface observed temperature anomalies of the seasonal and annual mean in Greece and Northern Hemisphere for the period 1979–2013. *Dashed* and *dotted lines* represent the trend lines

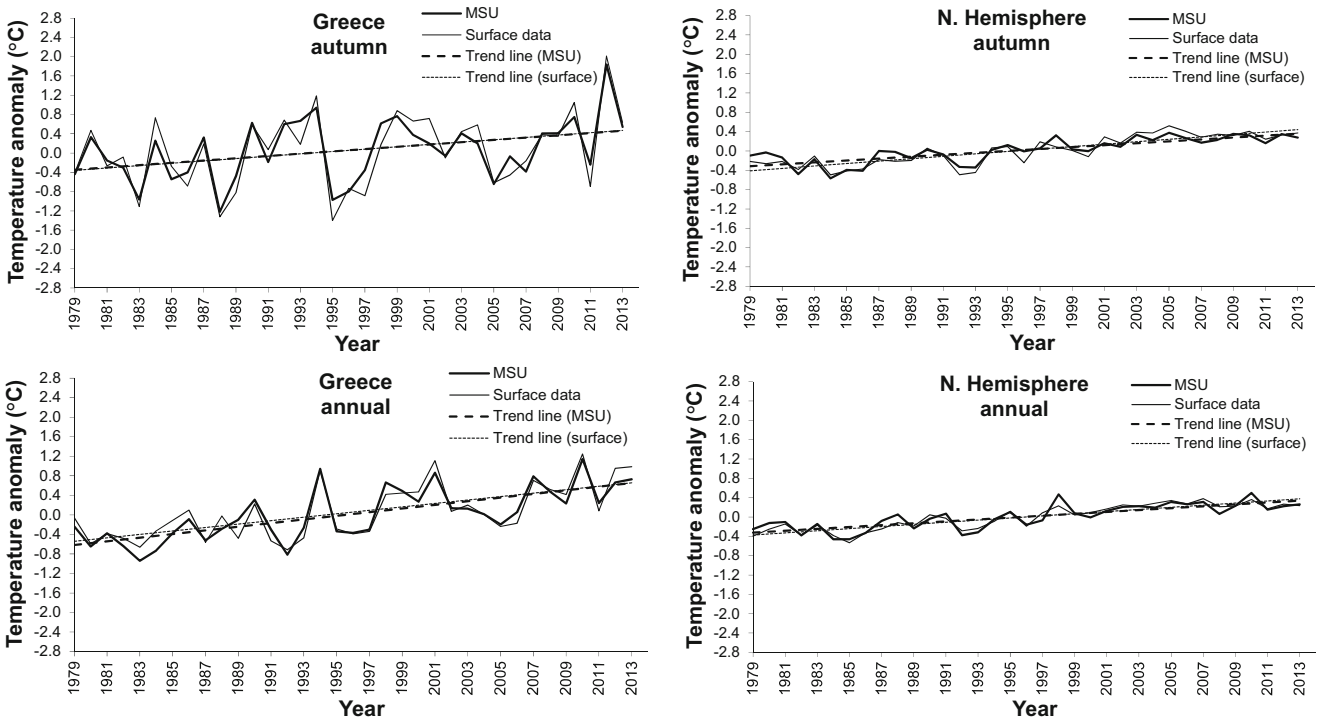

Fig. 6 (continued)

Time series of satellite and surface temperature anomalies match quite well (Fig. 6) with correlation coefficients ranging between 0.83 and 0.95 and mean absolute differences around 0.1 °C for NH and 0.15–0.35 °C for Greece (Table 8). Best agreement is obtained for annual time series and worst for winter.

3.3 Relationship of air temperature with circulation indices

One of the main objectives of this study is to investigate the link between atmospheric circulation and air temperature over Greece. First, the correlation of air temperature, at the national scale, with each of the five atmospheric circulation indices (NAOI, MOI, MCI, EMPI and NCPI) was examined (Table 9).

According to Table 9, three indices (NAOI, MOI, and MCI) present a significant negative correlation only with winter air temperature in Greece. Concerning the EMPI and NCPI, a slightly good correlation (statistically significant at 95 % confidence level) is set up in (almost) all seasons and especially in winter. These findings are in agreement with the results found by Kutiel et al. (2002) and Nastos et al. (2011) for previous periods.

The NCPI presents a distinctly higher negative correlation (−0.72) with winter temperatures compared to the other indices, followed by the Mediterranean oscillation indices MCI (−0.57), EMPI (−0.52) and MOI (−0.48). The NAOI provides the poorest correlation coefficient (−0.36) among the five indices, with the proportion of explained variance being up to

Table 8 Values of the correlation coefficient and the mean absolute difference between the satellite induced (MSU) tropospheric temperature anomalies and observed surface air temperature anomalies for Greece and the Northern Hemisphere for the period 1979–2013

	Winter	Spring	Summer	Autumn	Annual
(a) Correlation coefficient					
Greece	0.87	0.94	0.90	0.93	0.95
Northern Hemisphere	0.83	0.88	0.88	0.92	0.94
(b) Mean absolute difference (°C)					
Greece	0.35	0.27	0.31	0.23	0.15
Northern Hemisphere	0.14	0.11	0.10	0.10	0.07

Table 9 Correlation coefficients of seasonal and annual correlation of air temperature in Greece with circulation indices. (*Italicized values* indicate a 95 % level of significance)

	Winter	Spring	Summer	Autumn	Annual
NAOI	*−0.36*	−0.08	−0.11	0.08	−0.18
MOI	*−0.48*	−0.13	0.12	−0.19	−0.20
MCI	*−0.57*	−0.10	−0.12	0.10	0.20
EMPI	*−0.52*	*−0.48*	*−0.48*	−0.15	*−0.39*
NCPI	*−0.72*	*−0.38*	*−0.45*	*−0.49*	*−0.58*

52 % for NCPI, 33 % for MCI, 27 % for EMPI, 23 % for MOI and only 13 % for NAOI.

Only NCPI and EMPI present statistically significant correlation with other seasonal and annual temperatures with correlation coefficients ranging between −0.38 and −0.58 (except EMPI in autumn with −0.15) and the proportion of explained variance in the range of 14–34 %.

The previous results suggest that both the NCPI and EMPI have a significant influence on the temperature regime in Greece and can be considered as a climatic forcing factor. The NCP atmospheric teleconnection is by far the most representative of the air temperature variability in Greece. This connection, however, is not only developed during winter, as expected, but is also present during the other seasons and for the annual temperatures. The NCPI is more appropriate for studying the relationship of winter, autumn and annual temperatures in Greece with pressure patterns whereas the EMPI correlates better with spring and summer temperatures.

As far as the NAO is concerned, it seems that this large-scale atmospheric oscillation cannot interpret the regional variability of air temperatures in Greece as satisfactorily as the Mediterranean oscillation in pressure patterns (MCI, EMPI and MOI), either at the surface or at upper levels.

The time series of circulation indices and winter temperature anomalies are illustrated in Fig. 7. It is evident that the NCPI accounts for a significant proportion of the winter temperature variance in Greece as a result of the considerable correlation (−0.72) of winter temperature with the NCP atmospheric oscillation (Fig. 7e). The Mediterranean oscillation in pressure patterns (MCI, EMPI, MOI) accounts for a less proportion of the winter temperature variability than the NCPI (Fig. 7b–d). On the contrary, NAO can explain only major cold periods (1973–1976, 1980–1983, 1989–1993, 2012) and major warm periods (1977–1979, 2009–2011) on decadal scales (Fig. 7a). The trend analysis of the pressure indices' time series resulted in statistically significant decreasing trend

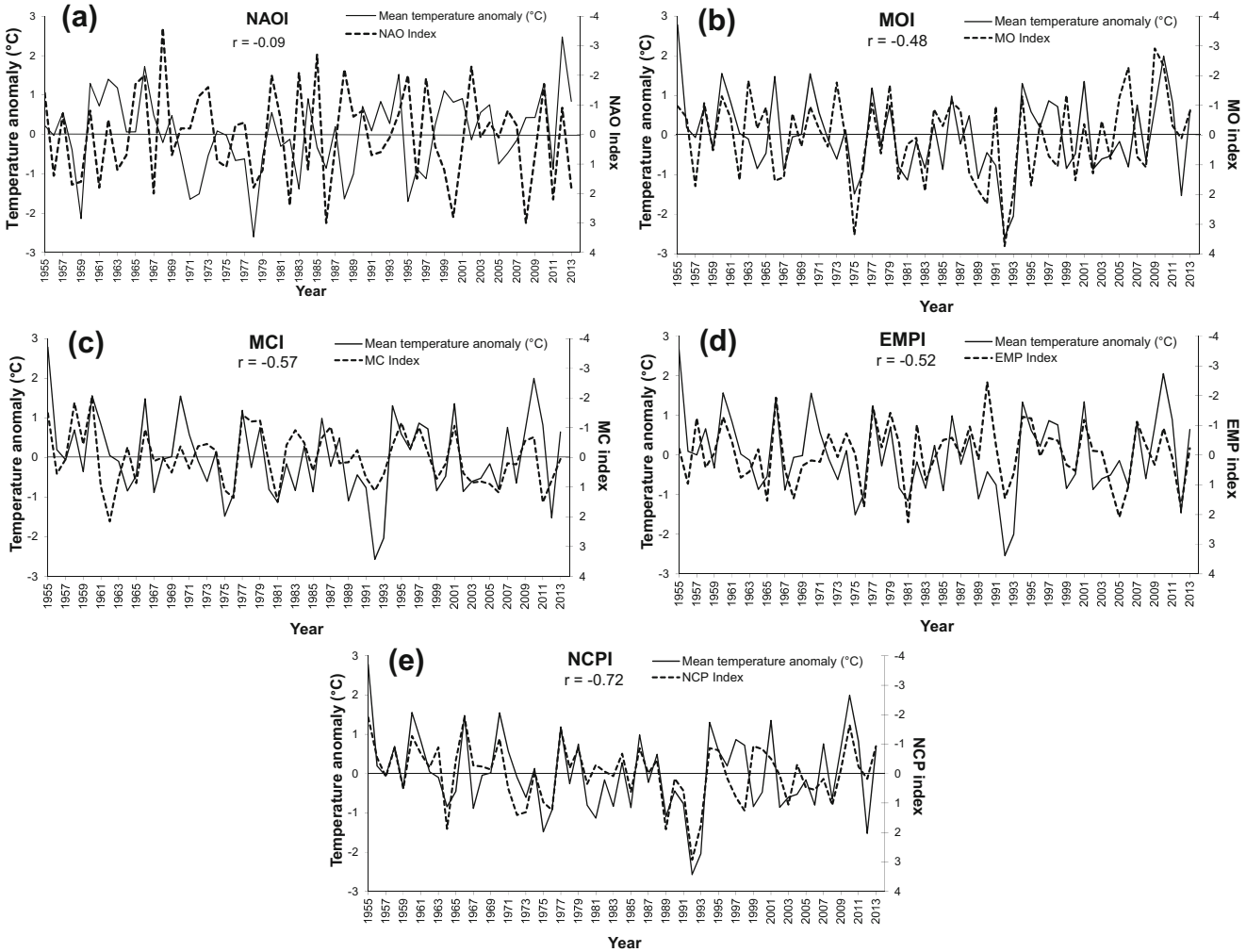

Fig. 7 Comparison between the winter temperature time series in Greece and circulation indices **a** NAOI, **b** MOI, **c** MCI and **d** EMPI and NCPI. Correlation coefficient *r* between them is also provided in the graphs

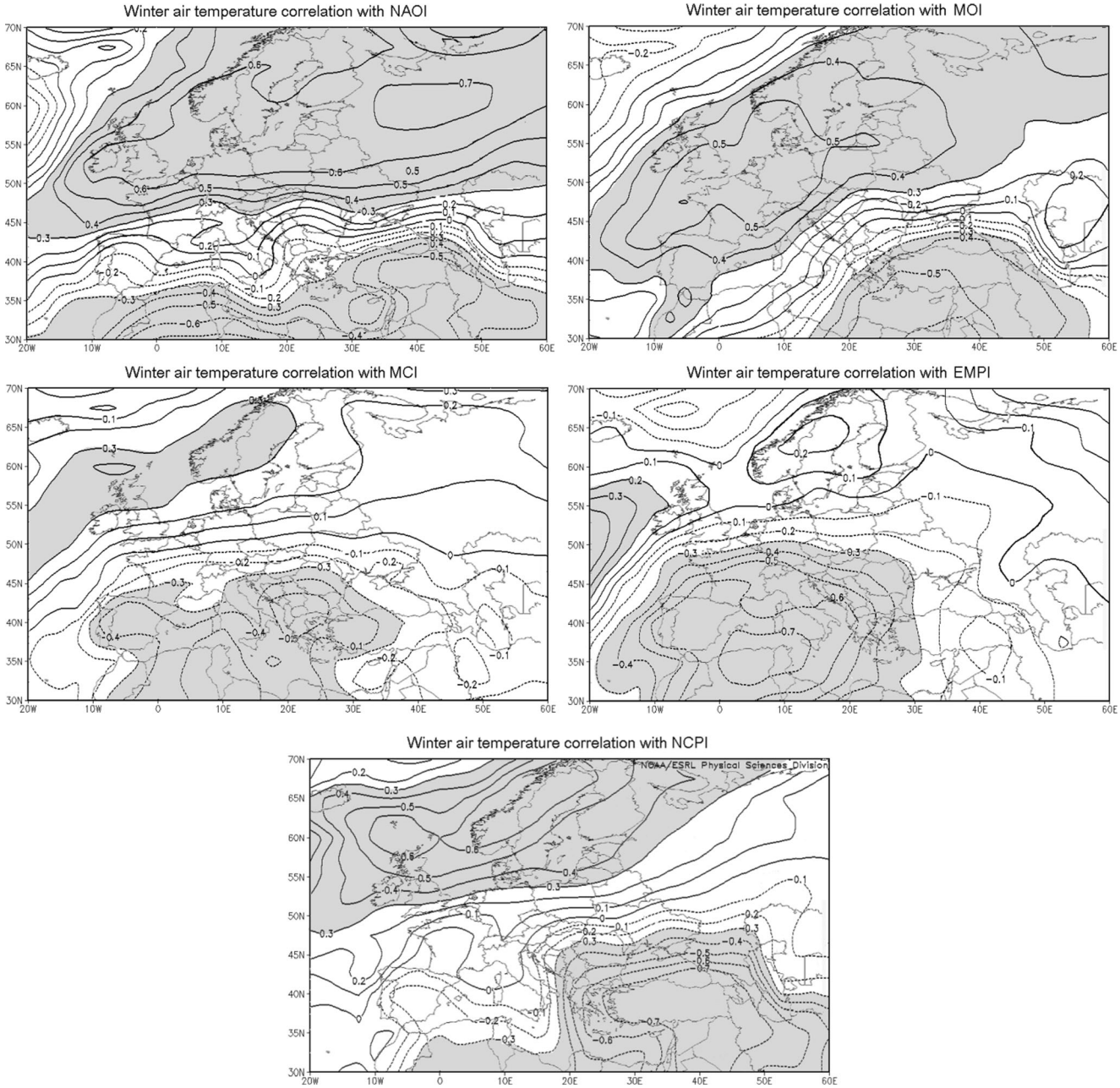

Fig. 8 Maps of winter air temperature correlation with the five indices (NAOI, MOI, MCI, EMPI and NCPI) for the period 1950–2013, using the monthly 2.5°×2.5° gridded reanalysis data of NCEP/NCAR. Statistically significant values at the 95 % level are highlighted with *light grey shades*

Table 10 Correlation coefficients among the five atmospheric circulation indices (*Italicized values* indicate a 95 % level of significance)

	NAOI	MCI	MOI	EMPI	NCPI
NAOI	–	0.24	*0.33*	0.16	*0.33*
MCI	0.24	–	0.24	*0.57*	*0.39*
MOI	*0.33*	0.24	–	−0.03	*0.44*
EMPI	0.16	*0.57*	−0.03	–	*0.28*
NCPI	*0.33*	*0.39*	*0.44*	*0.28*	–

only for the summer, autumn and annual time series of the EMPI and autumn and annual time series of the MCI. Only the increasing trend of the summer air temperature in Greece can be explained by the significant decreasing trend of the EMPI time series.

Figure 8 shows the spatial distribution of correlation between the winter air temperature and the five indices (NAOI, MOI, MCI, EMPI and NCPI) using the monthly 2.5°×2.5° gridded reanalysis data of NCEP/NCAR data for the period 1955–2013. These maps can be categorized in two groups with similar spatial distribution patterns of correlation.

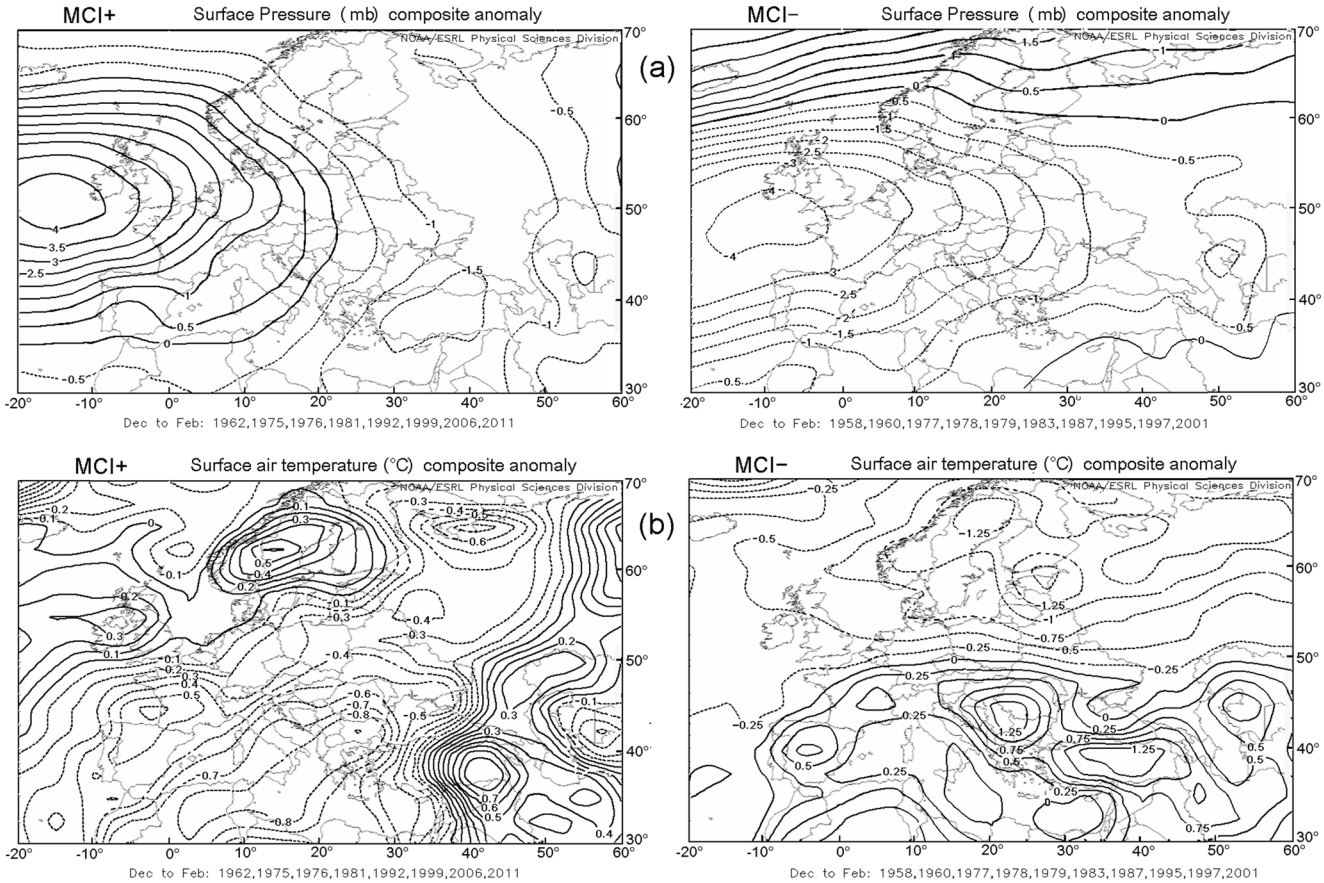

Fig. 9 Maps of composite anomalies (for 1955–2013) of (a) the sea level surface pressure (SLP) and (b) the surface air temperature during winter for selected years of positive and negative MCI values

The first group comprises the NAOI, MOI and NCPI with negative correlation coefficients over the southern and south-eastern Mediterranean and positive correlation coefficients prevailing over northern Europe. The NAOI presents a zonal distribution of correlation coefficients with the largest negative correlation (around −0.05) covering the southern and south-eastern Mediterranean as well as Turkey and Middle East. The highest positive correlation (0.7) is found over Russia. The correlation coefficients for MOI shows a similar to NAOI spatial distribution pattern with negative values (around −0.5), however, restricted to eastern and south-eastern Mediterranean as well as Turkey and Middle East and positive values extended to western Mediterranean. The NCPI seems to explain better the winter temperature variability over eastern and south-eastern Mediterranean, especially over Turkey and Middle East where negative correlation coefficients reach the value of −0.7, accounting for around 50 % of winter temperature variance. Greece is located at the edges of the area with statistically significant negative correlation coefficients (from −0.3 to −0.4 for NAOI, from −0.3 to −0.5 for MOI and from −0.5 to −0.7 for NCPI).

The second group consists of the regional scale indices MCI and EMPI with a pronounced negative correlation pole over the Mediterranean and weak positive correlations over the northwestern Atlantic. The MCI explains better the winter temperature variability (but only 25 %) over the Balkans, with correlations around −0.5 whereas the EMPI interprets better the temperature variance over the central-western Mediterranean (around 50 %) with correlation coefficients reaching the value of −0.7. Both indices explain approximately the same proportion of winter temperature variability over Greece.

The previous categorization of the circulation indices is verified when correlation among the winter indices is considered (Table 10). All three indices of the first group (NAOI, MOI and NCPI) are correlated with each other at the 95 % significance level, with MOI and NCPI being best correlated (0.44) and NAOI presenting a rather poor correlation (0.33) with the other indices. This supports the assumption made by Kutiel and Benaroch (2002) that the NCP is probably partly responsible for circulation modes over the Mediterranean such as the MOI. Concerning the other two indices (EMPI and MCI) of the second group, the high correlation (0.57) found between them points out a significant relationship between the upper level EMP and the surface MC which may be attributed to the southern EMP pole (Hatzaki et al. 2007).

Selected extreme positive and negative values of the three indices NCPI, EMPI and MCI (labelled by the respective year) were used to construct maps of the circulation at the respective atmospheric level as composite anomalies from the mean of the period 1955–2013, using the NCAR/NCEP data (Figs. 10 to 12). These three indices were chosen because they correlate best with the winter temperatures in Greece. Maps with the surface winter air temperature composite anomalies were also constructed for comparison.

An examination of Figs. 10 to 12 can explain in physical terms the relationship between temperature variance over Greece and regional (EMPI and MCI) and large-scale (NCPI) pressure patterns. In winters with positive (negative) MCI values, a centre of strong positive (negative) SLP anomalies prevails over northeastern Atlantic affecting the western-central Mediterranean, whereas negative (positive) anomalies are dominant over the eastern and south-eastern Mediterranean (Fig. 9a). This sets up a strong meridional pressure gradient which induces an enhanced frequency of dry and cold (humid and warm) northeasterly (southwesterly) airflow over Mediterranean. Consequently, during positive (negative) MCI values, winter in the Mediterranean and especially in Balkans tends to be significantly cooler (warmer) than the average (Fig. 9b).

A positive EMPI in winter is the result of a strong positive upper circulation anomaly prevailing over northeastern Atlantic and a negative anomaly in the eastern Europe extended over the eastern Mediterranean (Fig. 10a) which induces an enhanced mid-tropospheric northerly meridional flow toward the central Mediterranean. This leads to lower temperatures than the normal all over the Europe and the Mediterranean (Fig. 10b). On the contrary, during a negative phase of the EMP, an intensified negative circulation anomaly is established over the whole Europe resulting in an increased zonal flow over the Mediterranean (Fig. 10a) and in high winter temperatures over the Europe and especially in Balkans (Fig. 10b).

During positive (negative) NCPI, an intensified anticyclonic (cyclonic) upper circulation anomaly in the North Sea and an increased cyclonic (anticyclonic) circulation anomaly north of the Caspian Sea (Fig. 11a) induce a northern cold (southwestern warm) air stream over Balkans and Turkey, resulting in the decrease (increase) of winter air temperature in these regions (Fig. 11b).

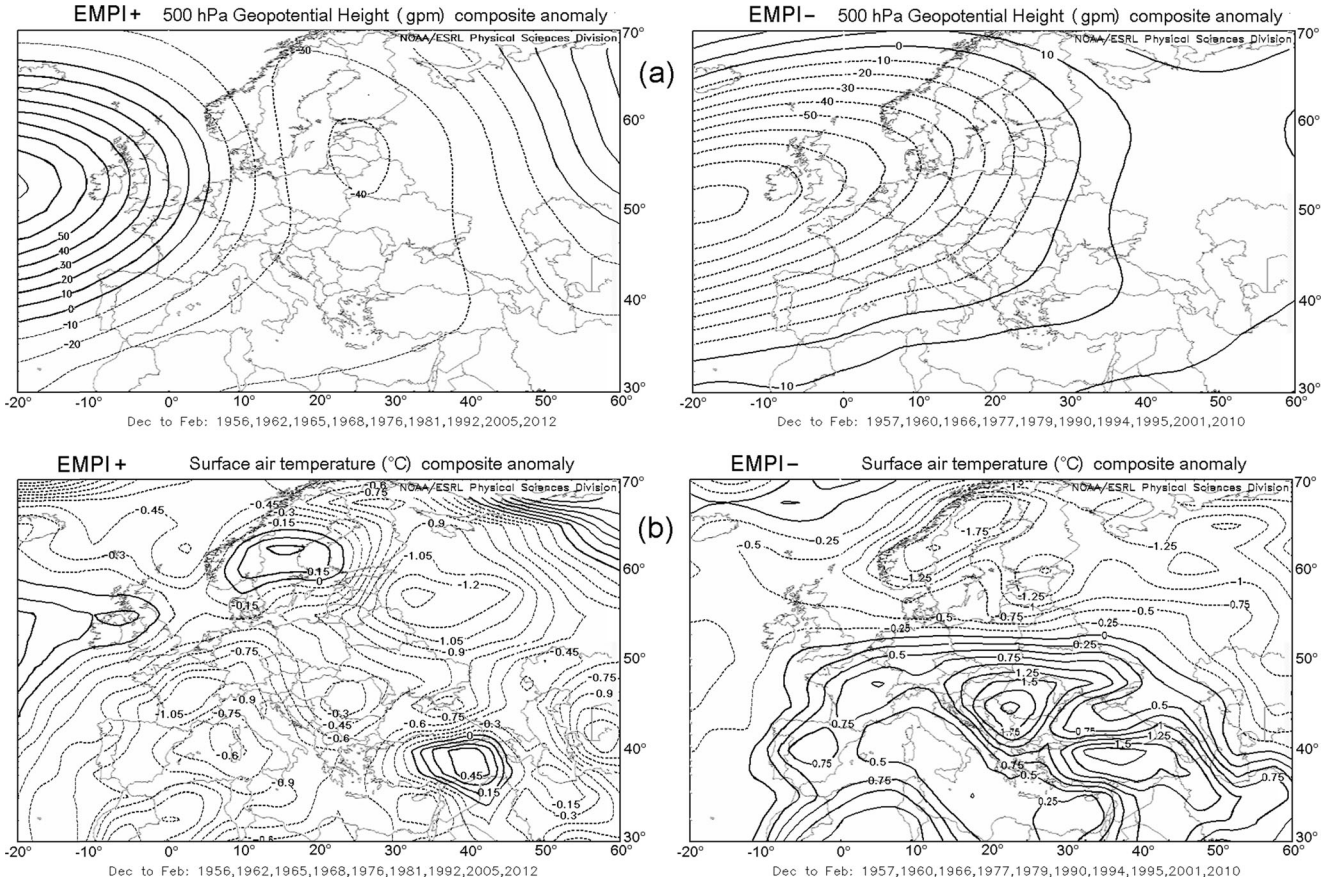

Fig. 10 Maps of composite anomalies (for 1955–2013) of **a** the geopotential height at the 500 hPa and **b** the surface air temperature during winter for selected years of positive and negative EMPI values

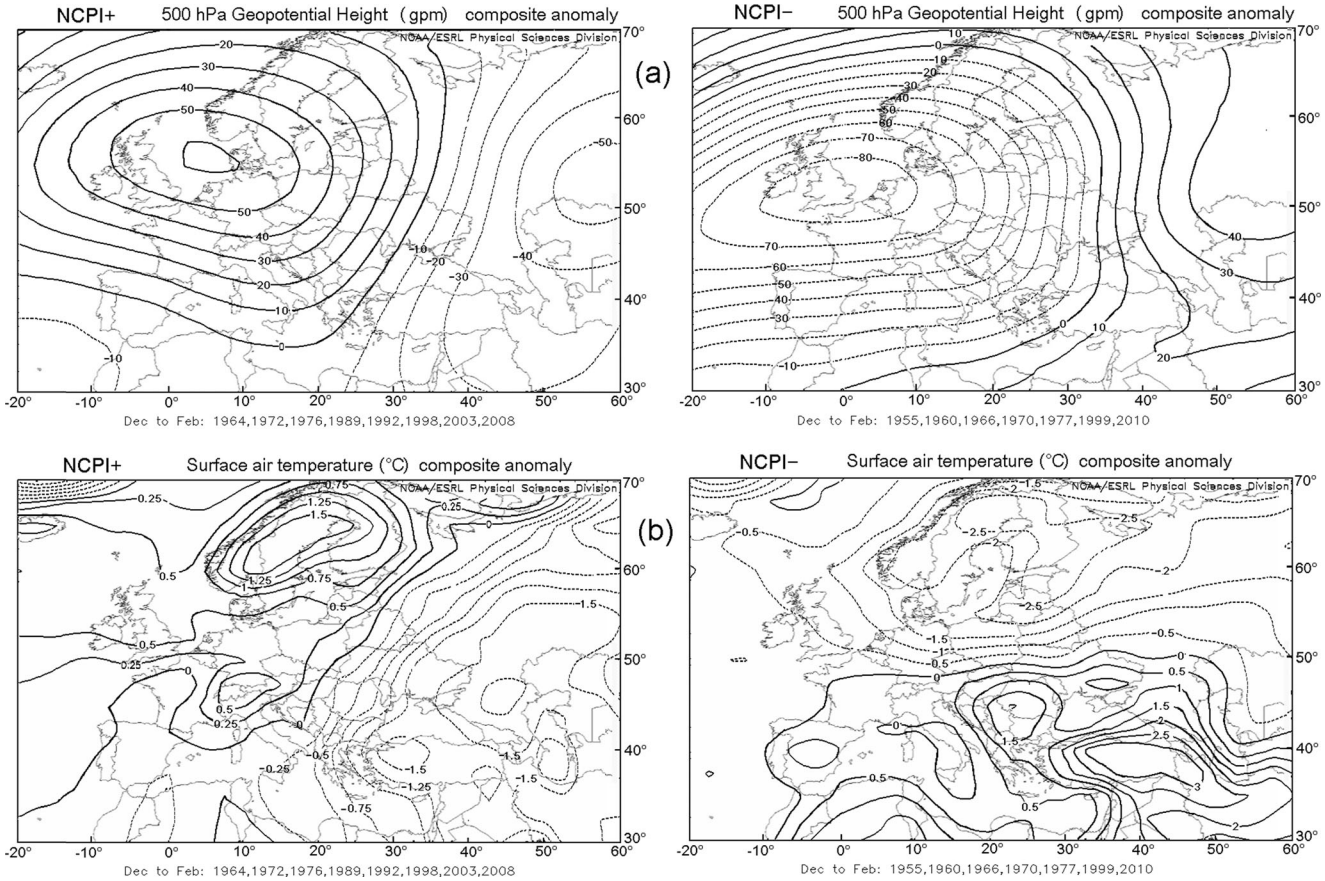

Fig. 11 Maps of composite anomalies (for 1955–2013) of **a** the geopotential height at the 500 hPa and **b** the surface air temperature during winter for selected years of positive and negative NCPI values

4 Conclusions

In this paper, the temperature trends at the surface and lower troposphere in Greece for the period 1955–2013 and their relationship to the atmospheric circulation were analysed, updating the study of Feidas et al. (2004) for data observed during the 12-year period 2002–2013. Trend analysis was based on a combination of three statistical tests.

Trend analysis of the annual and seasonal surface temperature time series updated to 2013 for 18 stations in Greece demonstrates some different results to those found in Feidas et al. (2004):

- The series updated to 2013 reveal a clearer positive trend than that presented in Feidas et al. (2004) for the period 1955–2001, on both the annual and the seasonal timescales. The warming signal detected previously only in summer has now intensified and spread in other seasons. Summer time series still exhibit a pronounced, strong warming trend for the majority of the stations. A statistically significant warming trend is also present in the half of the stations for spring and annual temperatures. In contrast, winter time series still show a general cooling trend but its statistical significance is now restricted to only one station.
- This warming signal appears to be mainly caused by the very high temperatures in the last decade (after 2004) of the record.
- At the national scale, there is now a better match between surface temperature trends in Greece and NH but only for summer, spring and annual time series, which are the only time series presenting a statistically significant warming trend in Greece. This is a result different from that found in the study of Feidas et al. (2004) according to which temperature trends in Greece and NH were not consistent for the period 1955–2001.
- In general, time series for both areas, Greece and NH, have a minimum lying around mid-1970s with the exception of winter in which the minimum for NH (late 1960s) and Greece (early 1990s) are not in agreement. This 25-year late response of winter temperatures in Greece to the recent NH warming seems to be the cause for the overall slight cooling trend observed in the winter series of Greece during the entire period 1995–2013.
- Identification of the approximate starting year of trend or an abrupt temperature change reveals that Greece exhibits

cooling trends in winter and autumn series, beginning in late 1950s and mid-1960s, respectively, which, however, seem to start reversing recently (2008–2013). A profound warming trend is evident in summer temperatures starting in mid-1990s, while spring and annual series entered into a period of a weaker warming trend one decade later (mid 2000s).

- Analysis of satellite-induced tropospheric temperature trends for the period 1979–2013 at the national and hemispheric scale reveals the following findings:

- All the satellite time series now show a statistically significant tropospheric temperature warming trend for both areas (Greece and NH). The magnitude of the warming trend found over Greece is, however, significantly larger than over the NH.
- Comparison of the lower tropospheric and surface temperature trends shows, in general, a very good agreement in both Greece and NH, with differences only in winter and summer for Greece.
- Time series of satellite and surface temperature anomalies correlate quite well with best agreement obtained for annual time series and worst for winter.

The investigation of the relationship between air temperature and five circulation indices (NAOI, MCI, MOI, EMPI and NCPI) provides evidence for the important role of atmospheric circulation in the behaviour of winter temperatures in Greece. The additional use of new indices such as EMPI and NCPI provides further insight into the relationship of regional atmospheric circulation and temperature variability. The new finding is that temperature trends are better explained by temporal changes in these two patterns of atmospheric circulation variability (EMP and NCP), mainly in winter. In particular:

- The correlation coefficients of air temperature with NAOI, MOI, and MCI are significant only in winter, due to the more coherent large-scale circulation typical for this season, whereas the EMPI and NCPI present a slightly good correlation with other seasonal and annual temperatures as well.
- The EMP and especially the NCP atmospheric teleconnection are by far the most representative of the air temperature variability in Greece. Thus, these two indices may be considered as the most appropriate for representing temperature variability in Greece. This connection, however, is not only developed during winter, as expected, but is also present for annual and other seasonal temperatures. The NCPI is more appropriate for studying the relationship between winter, autumn and annual temperatures in Greece and pressure patterns whereas the EMPI correlates better with spring and summer temperatures.
- The large-scale atmospheric oscillation of NAO cannot interpret satisfactorily the temperature variability in Greece.
- Although atmospheric pressure indices can explain a high proportion of temperature variance in Greece, there is not a distinct link between pressure indices and temperature in terms of trends. Only the positive trend of the summer air temperature in Greece has been found to be explained by a significant decreasing trend of the EMPI time series.

The link between temperature variability over Greece and regional (EMPI and MCI) and large-scale (NCPI) atmospheric teleconnection patterns was also physically explained. A positive EMPI and MCI in winter is linked to a dipole-like synchronous strengthening of a positive and a negative anomaly of mid-troposphere geopotential heights (or SLP) which induces an enhanced northerly meridional flow towards the Mediterranean. In contrast, a negative EMPI and MCI results to a meridional flow of southerly component and to a zonal flow, respectively. Consequently, during positive (negative) EMP and MC phases, lower (higher) temperatures than the normal occur over the Mediterranean. Similarly, during positive (negative) NCP phases, a northern cold (southwestern warm) air stream establishes over Balkans and Turkey, resulting in the decrease (increase) of winter air temperatures in these regions.

References

Ageena I, Macdonald N, Morse AP (2014) Variability of maximum and mean average temperature across Libya (1945-2009). Theor Appl Climatol 117(3–4):549–563

Alexandersson H (1986) A homogeneity test applied to precipitation data. J Climatol 6:661–675

Allen RG, Pereira LS, Raes D, Smith M (1998) Statistical analysis of weather data sets. In: Crop evapotranspiration–guidelines for computing crop water requirements, FA–Food and Agriculture Organization of the United Nations (Ed.), Annex IV, FAO Irrigation and drainage paper 56, Rome: FAO

Bajat B, Blagojević D, Kilibarda M, Luković J, Tošić I (2015) Spatial analysis of the temperature trends in Serbia during the period 1961–2010. Theor Appl Climatol 121(1–2):289–301

Barnston A, Livezey R (1987) Classification, seasonality and persistence of low-frequency atmospheric circulation patterns. Mon Weather Rev 115:1083–1126

Bloomfield P, Nychka DW (1992) Climate spectra and detecting climate change. Climate Change 21:275–287

Brunet M, Jones PD, Sigro J, Saladie O, Aguilar E, Moberg A, Della-Marta PM, Lister A, Walther D, Lopez D (2007) Spatial and temporal temperature variability and change over Spain during 1850–2003. J Geophys Res 112:D12117

Brunetti M, Maugeri M, Nanni T (2002) Atmospheric circulation and precipitation in Italy for the last 50 years. Int J Climatol 22:1455–1471

Brunetti M, Kutiel H (2011) The relevance of the North-Sea Caspian Pattern (NCP) in explaining temperature variability in Europe and the Mediterranean. Nat Hazards Earth Syst Sci 11:2881–2888

Christy JR, Norris WB, Spencer RW, Hnilo JJ (2007) Tropospheric temperature change since 1979 from tropical radiosonde and satellite measurements. J Geophys Res 112: D06102

Colacino M, Conte M (1993) Greenhouse effect and pressure patterns in the Mediterranean basin. Il NuovoCimento C 16:67–76

Conte M, Giuffrida S, Tedesco S (1989) The Mediterranean oscillation: impact on precipitation and hydrology in Italy. Proc. Conference on Climate and Water, vol. 1, Academy of Finland 9:1989. 121–137

Criado-Aldeanueva F, Soto-Navarro FJ (2013) The Mediterranean oscillation teleconnection index: station-based versus principal component paradigms. Adv. Meteorolvol 2013, Article ID 738501, 10 pages, doi: 10.1155/2013/738501

del Río S, Herrero L, Pinto-Gomes C, Penas A (2011) Spatial analysis of mean temperature trends in Spain over the period 1961–2006. Glob Planet. Chang 78(1–2):65–75

Douguedroit A (1998) Que peut-on dire d'une oscillation Méditerranéenne ? In climate and environmental change, Alcoforado MJ (ed.). Evora: 135–136

Feidas H, Makrogiannis T, Bora-Senta E (2004) Trend analysis of air temperature time series in Greece and their relationship with circulation using surface and satellite data: 1955–2001. Theor Appl Climatol 79:185–208

Goosens Ch, Berger A (1986) Annual and seasonal climatic variations over the Northern Hemisphere and Europe during the last century. Ann Geophys B 4(4):385–400

Grenander U (1954) On the estimation of regression coefficients in the case of autocorrelated disturbance. Ann Math Stat 29:252–272

Gryer JD (1986) Time series analysis. Duxbury Press, Belmont, California, 286 pp

Hasanean H, Abdel Basset H (2006) Variability of summer temperature over Egypt. Int J Climatol 26:1619–1634

Hatzaki M, Flocas HA, Asimakopoulos DN, Maheras P (2007) The eastern Mediterranean teleconnection pattern: identification and definition. Int J Climatol 27:727–737

Hatzaki M, Flocas HA, Giannakopoulos C, Maheras P (2009) The impact of the eastern Mediterranean teleconnection pattern on the Mediterranean climate. J Clim 22(4):977–992

Hurrell JW (1995) Decadal trends in the North Atlantic oscillation: regional temperatures and precipitation. Science 269:676–679

IPCC (1996) Climate change 1995: the science of climate change: contribution of Working Group I to the Second Assessment Report of the Intergovernmental Panel on Climate Change. Cambridge University Press, Cambridge

IPCC (2013) Climate change 2013: the physical science basis. In Working Group I Contribution to the Intergovernmental Panel on Climate Change Fifth Assessment Report (AR5)–changes to the underlying scientific/technical assessment. Cambridge University Press, Cambridge and New York

Jones PD, Lister DH, Osborn TJ, Harpham C, Salmon M, Morice CP (2012) Hemispheric and large-scale land surface air temperature variations: an extensive revisionand an update to 2010. J Geophys Res 117:D05127

Jones PD, Moberg A (2003) Hemispheric and large-scale surface air temperature variations: an extensive revision and an update to 2001. J Clim 16:206–223

Kalnay E, Kanamitsu M, Kistler R, Collins W, Deaven D, Gandin L, Iredell M, Saha S, White G, Woollen J, Zhu Y, Leetmaa A, Reynolds R, Chelliah M, Ebisuzaki W, Higgins W, Janowiak J, Mo KC, Ropelewski C, Wang J, Jenne R, Joseph D (1996) The NCEP/NCAR 40-year reanalysis project. Bull Am Meteorol Soc 77:437–470

Knezevic S, Tosic I, Unkasevic M, Pejanovic G (2014) The influence of the East Atlantic oscillation to climate indices based on the daily minimum temperatures in Serbia. Theor Appl Climatol 116(3–4): 435–446

Kutiel H, Maheras P, Guika S (1996) Circulation and extreme rainfall conditions in the eastern Mediterranean during the last century. Int J Climatol 16:73–92

Kutiel H, Maheras P (1998) Variations in the temperature regime across the Mediterranean during the last century and their relationship with circulation indices. Theor Appl Climatol 61:39–53

Kutiel H, Benaroch Y (2002) North Sea Caspian Pattern (NCP)–an upper level atmospheric teleconnection affecting the eastern Mediterranean: identification and definition. Theor Appl Climatol 71:17–28

Kutiel H, Maheras P, Türkes M, Paz S (2002) North Sea Caspian pattern (NCP)–an upper level atmospheric teleconnection affecting the eastern Mediterranean: implications on the regional climate. Theor Appl Climatol 72:173–192

Kutiel H, Türkeş M (2005) New evidence for the role of the North Sea–Caspian Pattern on the temperature and precipitation regimes in continental central Turkey. Geogr Ann Ser A Phys Geogr 87:501–513

Kutiel H, Brunetti M (2010) The role of the North-Sea Caspian Pattern (NCP) on temperature variability in Europe and the Mediterranean. Plinius Conference Abstracts, Vol. 12, Plinius 12–52

Longobardi A, Mautone M (2015) Trend analysis of annual and seasonal air temperature time series in Southern Italy. Engineering geology for society and territory, vol 3: River basins, reservoir sedimentation and water resources, 501–504

Luterbacher J, Xoplaki E, Burgard R., Schmutz C (2000) Connection between the large scale lower atmospheric circulation and the winter temperature variability over Greece: 1957–1997. Proc. 5th Greek Scientific Conference In Meteorology-Climatology-Atmospheric Physics. Athens, 28–30 September 1998. 81–88 pp

Maheras P, Xoplaki E, Kutiel H (1999) Wet and dry monthly anomalies across the Mediterranean basin and their relationship with circulation, 1860-1990. Theor Appl Climatol 64:189–199

Maheras P, Kutiel H (1999) Spatial and temporal variations in the temperature regime in the Mediterranean and their relationship with circulation during the last century. Int J Climatol 19:745–764

Marougianni G, Melas D, Kioutsioukis I, Feidas H, Zanis P, Anadranistakis E (2012) Trend analysis of climatic time series for Greece. In Helmis CG, Nastos P (eds) Advances in meteorology, climatology and atmospheric physics. Springer, Berlin, Heidelberg, vol 1, pp. 583–589, ISBN 978–3–642-29171-5

Mitchell T, Hulme M (2000) A country-by-country analysis of past and future warming rates. Tyndall Centre Internal Report. No. 1. November, UEA, Norwich, UK. Cited in: https://crudata.uea.ac.uk/~timm/papers/

Michell JM, Dzerdzeevskii B, Flohn H, Hofmeyr WL, Lamb HH, Rao KN, Walléen CC (1966) Climatic change. WMO Tech. Note 79, WMO No. 195. TP-100. Geneva, 79 pp

Nastos PT, Philandras CM, Founda D, Zerefos CS (2011) Air temperature trends related to changes in atmospheric circulation in the wider area of Greece. Int J Remote Sens 32(3):737–750

Nicholls N, Cruza GV, Jourel J, Karl TR, Ogallo LA, Parker DE (1996) Observed climate variability and change. In: Houghton JT, and others (eds). Climate change 1995: the science of climate change. Report of IPCC Working Group I, Cambridge: University Press, 137–192

Parker DE, Jones PD, Folland CK, Bevan A (1994) Interdecadal changes of surface temperature since the late nineteenth century. J Geophys Res 99:14373–14399

Peterson TC, Easterling DR, Karl TR, Groisman P, Nicholls N, Plummer N, Torok S, Auer I, Boehm R, Gullett D, Vincent L, Heino R, Tuomenvirta H, Mestre O, Szentimrey T, Salinger J, Førland EJ, Hanssen-Bauer I, Alexandersson H, Jones P, Parker D (1998) Homogeneity adjustments of in situ atmospheric climate data: a review. Int J Climatol 18:1493–1517

Piervitali E, Colasino M, Conte M (1997) Signals of climatic change in the Central-Western Mediterranean Basin. Theor Appl Climatol 58: 211–219

Piervitali E, Colasino M, Conte M (1999) Rainfall over the central-western Mediterranean basin in the period 1951-1995. Part II: precipitation scenarios. Il Nuovo Cimento C 22:649–661

Proedrou M, Theoharatos G, Cartalis C (1997) Variations and trends in annual and seasonal air temperature in Greece determined from ground and satellite measurements. Theor Appl Climatol 57:65–78

Retalis D, Hatzioannou L, Pasiardis S, Nikolakis D, Asimakopoulos DN, Lourantos N (1998) Study of the temperature time series in SE Greece and Cyprus. (in Greek) Proc. 4th Greek Scientific Conference in Meteorology-Climatology-Atmospheric Physics. Athens, 22–25 September 1998. 271–278

Rogers JC, van Loon H (1979) The seesaw in winter temperatures between Greenland and northern Europe. Part II: some oceanic and atmospheric effects in middle and high latitudes. Mon Weather Rev 107:509–519

Saaroni H, Ziv B, Edelson J, Alpert P (2003) Long term variations in summer temperature over the eastern Mediterranean. Geophys Res Lett 30:1946

Sahsamanoglou HS, Makrogiannis TJ (1992) Temperature trends over the Mediterranean region, 1950-1988. Theor Appl Climatol 45: 183–192

Sneyers R (1990) On the statistical analysis of series of observations. Tech. Note 143, WMO No. 415, Geneva, 192 pp

Sušelj K, Bergant K (2006) Mediterranean oscillation index. Geophysical research abstracts, Vol. 8, 02145, 2006 SRef-ID: 1607-7962/gra/EGU06-A-02145

Türkeş M, Sumer UM, Demir I (2002) Re-evaluation of trends and changes in mean, maximum and minimum temperatures of Turkey for the period 1929–1999. Int J Climatol 22:947–977

Türkeş M, Erlat E (2009) Winter mean temperature variability in Turkey associated with the North Atlantic Oscillation. Meteorog Atmos Phys 105(3–4):211–225

Van Loon H, Rogers JC (1978) The seesaw in winter temperatures between Greenland and northern Europe. Part I: winter. Mon Weather Rev 104:365–380

Walker GT (1924) Correlations in seasonal variations of weather. IX. Mem Indian Meteorol Dep 24:275–332

Walker GT, Bliss E (1932) World weather V. Mem R Meteorol Soc 4:53–84

WMO (2009) Handbook on CLIMAT and CLIMAT TEMP reporting. World Meteorological Organization, World Weather Watch Technical Report, WMO/TD-No. 1188

Xoplaki E, Gonzalez-Rouco FJ, Gyalistras D, Luterbacher J, Wanner H (2003) Mediterranean summer air temperature variability and its connection to the large-scale atmospheric circulation and SSTs. Clim Dyn 20:723–739